N. Jb. Geol. Paläont. Abh. 271/3 (2014), 285–306
Stuttgart, March 2014 **Article**

Triassic Paleo-Tethys subduction in the center of the Alpine-Himalayan Orogen: Evidence from Dehnow I-type granitoids (NE Iran)

Ramin Samadi, Esteban Gazel, Hassan Mirnejad, Hiroshi Kawabata, Ali Akbar Baharifar and Seyed Jamal Sheikh Zakariaee

With 9 figures and 3 tables

Abstract: The granitoids of Dehnow in NE Iran are part of a calc-alkaline plutonic series (diorite-tonalite-granodiorite) that intruded the remnants of the Paleo-Tethys oceanic crust during the Triassic. New major and trace element data together with isotopic compositions elucidate their I-type nature and a deep magma origin. P-T calculations based on amphibole and plagioclase suggest crystallization stages in the upper lithosphere at an approximate pressure of 6.4 kbar and temperature of 708 °C. The Dehnow granitoids are characterized by high concentrations of LILE, LREE, HFSE and low concentrations of HREE, similar to some worldwide I-type granites, including examples from Harsit (along the Alpine-Himalayan suture zone), Iberia and the Martins Pereira plutons. The new geochemical data in combination with mineral parageneses and field observations suggest that the origin of the low temperature, Caledonian-type, arc-related granitoids of Dehnow resulted from the subduction of the Paleo-Tethys oceanic slab beneath the Turan block (along the Alpine-Himalayan suture zone) and involved the contribution of lower crust and mantle melts in this collisional setting.

Key words: I-type granitoids, Alpine-Himalayan Orogen, Dehnow pluton, Iran.

Introduction

As a major component of the continental crust, granitoids provide important clues on lithospheric evolution and tectonics. They originate from a wide range of source settings from mantle to upper crust and show various magma evolutions. For many years, genesis and classification of granites were the main themes of many publications (e.g. Chappell & White 1974; Barbarin 1999; Frost et al. 2001, etc.). A fundamental subdivision between I- and S-types was proposed by Chappell & White (1974) on the basis of petrographic and geochemical characteristics of the Lachlan Fold Belt (LFB) granitoids, southeastern Australia. S-Types are interpreted to result from partial melting of metasedimentary source rocks, a process called anatexis. I-type granites are produced either directly by fractional crystallization of mantle-derived liquids, direct partial melting of mantle-derived source rocks in the crust, or melting of mantle modified by silicic melts (pyroxenitic veins). Therefore, the source materials for I-type granites are broadly basaltic to andesitic in composition (Chappell & White 1992; Pitcher 1993). Characteristics of I- and S-type granites are available in Table 8.3.1 in Gill (2010). One important contrasting feature of S-type granites is that they are always peraluminous with excess Al hosted in Al-rich biotite, cordierite, or muscovite. In comparison, the least felsic I-type granites are metaluminous (some weakly peraluminous) while their excess Al is a function of the melting process, and unrelated to the bulk composition of the source (Chappell et al. 2012). Chappell & White (1984, 1992) and Chappell et al. (1998) confirmed the I- and S-types subdivision and proposed

www.schweizerbart.de
DOI: 10.1127/0077-7749/2014/0390
0077-7749/2014/0390 $ 5.50

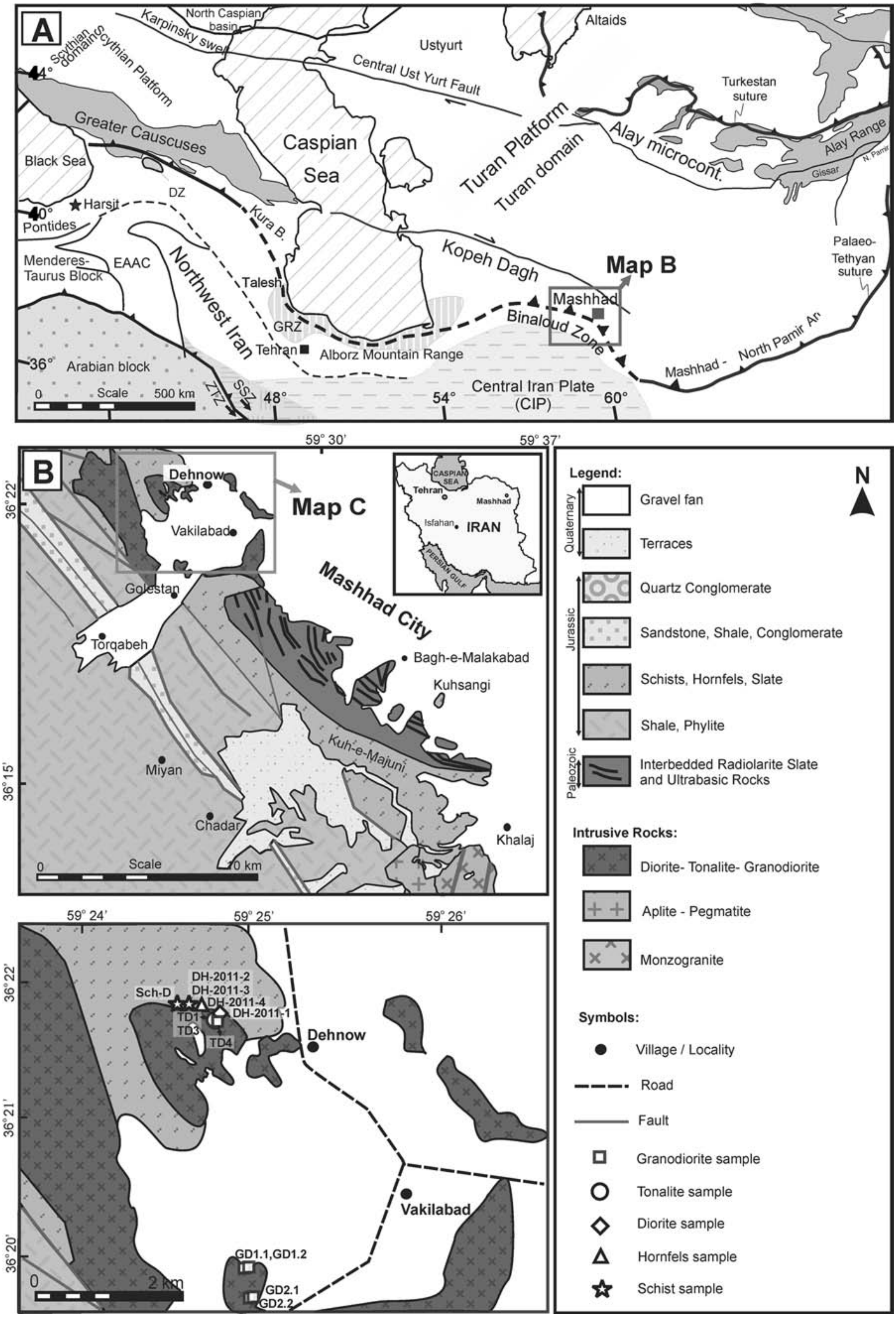
A
North Caspian basin
Karpinsky swell
Scythian domains
Scythian Platform
Ustyurt
Altaids
Central Ust Yurt Fault
Turkestan suture
Greater Causcuses
Caspian Sea
Turan Platform
Turan domain
Alay microcont.
Alay Range
Gissar
N. Pamir
Black Sea
Harsit
DZ
Pontides
Kura B.
Menderes-Taurus Block
EAAC
Northwest Iran
Talesh
Kopeh Dagh
Map B
Palaeo-Tethyan suture
Mashhad
Binaloud Zone
GRZ
Tehran
Alborz Mountain Range
Mashhad - North Pamir Arc
Arabian block
Central Iran Plate (CIP)
Scale
500 km
ZFZ
SSZ
44°
40°
36°
48°
54°
60°
B
59° 30'
59° 37'
36° 22'
36° 15'
Dehnow
Vakilabad
Map C
Golestan
Torqabeh
Mashhad City
Bagh-e-Malakabad
Kuhsangi
Kuh-e-Majuni
Miyan
Chadar
Khalaj
Scale
10 km
CASPIAN SEA
Tehran
Mashhad
Isfahan
IRAN
PERSIAN GULF
Legend:
N
Quaternary
Gravel fan
Terraces
Jurassic
Quartz Conglomerate
Sandstone, Shale, Conglomerate
Schists, Hornfels, Slate
Shale, Phylite
Paleozoic
Interbedded Radiolarite Slate and Ultrabasic Rocks
Intrusive Rocks:
Diorite- Tonalite- Granodiorite
Aplite - Pegmatite
Monzogranite
Symbols:
Village / Locality
Road
Fault
Granodiorite sample
Tonalite sample
Diorite sample
Hornfels sample
Schist sample
59° 24'
59° 25'
59° 26'
36° 22'
36° 21'
36° 20'
Sch-D
DH-2011-2
DH-2011-3
DH-2011-4
DH-2011-1
TD1
TD3
TD4
Dehnow
Vakilabad
GD1.1,GD1.2
GD2.1
GD2.2
2 km

Fig. 1.

that I-type granites occur as two distinct groups, high- and low-temperature, based on the absence or presence of inherited zircons, respectively. The "high-temperature" I-type granites are the most primitive and form by partial melting of mafic rocks in the deep crust, or perhaps in subduction-modified mantle at temperatures higher than 1000 °C (Chappell et al. 1998), and are dominantly high-Ca tonalitic to low-K granodioritic rocks. These granites, called Cordilleran I-type, occur in younger subduction-related continental margins (Pitcher 1993). The "low temperature" granites formed by partial melting of quartzo-feldspathic crust at low magmatic temperatures of ~700-800 °C (Chappell et al. 1998). Low-temperature I-type granites, known as Caledonian I-type, are commonly associated with S-type granites (Pitcher 1993).

Plutonic rocks of diverse compositions crop out in Iran (Berberian 1981, Haghipour & Aghanabati 1989), particularly in the Central Iran Plate (CIP) and the Sanandaj-Sirjan Metamorphic Zone (in the NW to SE of Iran) (Jamshidi-Bahr et al. 2013). Distinct granitoid suites, i.e., monzogranite, granodiorite, tonalite, and diorite, occur in the Mashhad area. While the large granodiorite and monzogranite intrusions make up the Mashhad batholiths, an isolated heterogeneous pluton comprising Diorite, Tonalite and Granodiorite (DTG) occurs in the Dehnow area. This pluton intruded pre-Late Triassic metamorphosed rocks and is characterized by a narrow contact aureole. Previous works considered the Mashhad granites to be part of the CIP (e.g. Soltani 2000), but Zanchi et al. (2011) included them in the Turan Platform. NE Iran is a key location for studying the Cimmerian Orogeny, which is the result of the Late Triassic collision between the CIP and Eurasia, and the closure of the Paleo-Tethys. Although recent analyses of the Cimmerian evolution have been performed in the Alborz Belt, studies in NE Iran are scarce (Zanchi et al. 2011). The Mashhad granitoids are a part of the Mashhad-Pamir Arc. Natalin & Sengor (2005) and Mirnejad et al. (2013) considered them as a part of the so-called Silk Road arc that extended for 8300 km along the entire southern margin of Eurasia from North China to Europe and formed as the result of north-dipping subduction of the Paleo-Tethys.

This study fills the missing gap of geochemical data of I-type granitoids from the Mashhad-Pamir arc in NE Iran. Here, we present new insights and reconsider the source and genesis of the Dehnow granitoids based on electron probe micro analyses (EPMA), X-ray fluorescence (XRF), and inductively coupled plasma mass spectrometry (ICP-MS) data. We also reevaluate the whole rock and isotope data of previous studies. In addition, a geochemical comparison was made between the granitoids of the Dehnow pluton and those I-type granite suites from Harsit, in the western portion of Alpine-Himalayan fold-and-thrust belt, Martins Pereira, Iberia and the Lachlan Fold Belt to better constrain the plutonic events related to the collision of the Turan and CIP via the closure of Paleo-Tethys in the center of the Alpine-Himalayan Orogen.

Geo-tectonic background

Iran is located in the middle of the Alpine-Himalayan Orogen and was produced by collision between the Eurasian Plate to the north, and the Afro-Arabian Plate to the southwest. The Alpine-Himalayan Orogen forms a continuous range of suture zones from the eastern Mediterranean to the NW Himalayan belt (Fig. 1A). The Binaloud Mountains that extend along the Paleo-Tethys suture of northern Iran are located in the southern part of the Kopeh Dagh zone (Turan Plate) and form a transition zone between the Alborz and Central Iran zones (Fig. 1A). During Mesozoic time, the convergence occurring between the CIP and Turan plate continued with NE trending compression that caused folding of older rocks in the Kopeh Dagh area. In the Binaloud area this deformation generated several SE to SW vergent thrust fault systems, resulting in the imbrication of Paleozoic and Mesozoic successions and Neogene sediments at the southern border of the Binaloud Mountains (Sheikholeslami & Kouh-

Fig. 1. A – Simplified main tectonic and orographic units from the Black Sea to Iran and the Pamir (modified after Natalin & Sengor 2005) (DZ: Dzurila massif, EAAC: East Anatolian Accretionary Complex (Late Cretaceous to Early Oligocene), SSZ: Sanandaj Sirjan Metamorphic Zone, ZTZ: Zagros Thrust Zone, GRZ: Gorgan Rasht Zone, CIP: Central Iran Plate). **B** – Geological map of the Mashhad area. **C –** Locations of the samples on the Dehnow geological map, NW of Mashhad city.

PEYMA 2012). The Paleo-Tethys suture zone includes meta-ophiolites and meta-flysch sequences. Tectonic reconstructions suggest that the Silurian opening of the Paleo-Tethys in northern Iran was followed by northward subduction beneath the Turan Plate (the southern part of Laurasia) in the Late Devonian, subsequent Cimmerian collision between the Iranian Microcontinent and Turan Plate, and obduction during the Late Triassic (ALAVI 1991; NATALIN & SENGOR 2005; KARIMPOUR et al. 2010). MAJIDI (1981) compared the meta-flysch with similar, but less metamorphosed, fossil-bearing rocks exposed 150 km southeast of Mashhad and suggested a Devonian-Carboniferous age for them. The meta-ophiolites and granites in the Mashhad area are surrounded by metamorphic rocks, consisting of well-layered slate, phyllite, schist, hornfels, marble, quartzite, and skarn (SAMADI et al. 2012, 2014). The Paleo-Tethys remnants (meta-ophiolite and meta-flysch) were intruded by granitic rocks in Triassic times (KARIMPOUR et al. 2010).

The Mashhad granitoids have been the focus of many studies (e.g. ALAVI & MAJIDI 1972; ALBERTI & MOAZEZ-LESCO 1974; MAJIDI 1978; MIRNEJAD et al. 2013). The Dehnow granitoids have been partly investigated by SAMADI (2009, 2014), VALIZADEH & KARIMPOUR (1995), KARIMPOUR et al. (2010) and MIRNEJAD et al. (2013). The Mashhad granitoid suites intruded a metamorphic complex. VALIZADEH & KARIMPOUR (1995) suggested that these intrusives belong to the S-type granites, and originated from the lower continental crust in the early stage of collision. Nevertheless, chemical analyses of different granitoid suites from the Mashhad area indicate metaluminous I-type and peraluminous S-type components (IRANMANESH & SETHNA 1998). MIRNEJAD et al. (2013) classified the granitoids of the Mashhad area into I- and S-type granites, related, respectively, to subduction and collision settings.

The Dehnow pluton intruded along the Paleo-Tethys suture and the outcrop is approximately 1 km by 2 km in size (Fig. 1A-B). This pluton is cross-cut by NW-SE trending shear zones exhibiting intense ductile deformation. Rocks along these shear zones include protomylonite, mylonite and ultra-mylonite with a steeply dipping mylonitic foliation and a gently plunging stretching lineation. These fabrics formed during the Cimmerian Orogeny between Late Triassic and Early Jurassic (RAHIMI & ALIZADEH 2010). The main lithological units in this area are diorite, tonalite, granodiorite, hornfels and micaschist. These lithologies are part of the NW-SE trending granitoid-metamorphic complexes cropping out in the west to south of the Mashhad area. The Dehnow granitoid was emplaced in the axial zones of second generation folds in low to medium grade metamorphosed pelitic, psammitic and carbonate rocks (MOAZEZ-LESCO & PLIMER 1979). SAMADI et al. (2012) indicate that the already-metamorphosed flysch and garnet micaschist of Dehnow have undergone metamorphic P-T conditions of ~5.3 kbar, ~569 °C under lower amphibolite facies conditions prior (to synchronous) with intrusion. Recent work by KARIMPOUR et al. (2010) proposed that the source of the Dehnow granitoids was continental crust (S-type granitoid), including metagreywacke to metapelite. MAJIDI (1983) dated the Dehnow granodiorite by the K-Ar method and reported ages of 211-215 Ma (Late Triassic, Norian). Later work by LAMMERER et al. (1984) and ALAVI (1991) suggested an Early Permian age (~256-245 Ma, based also on K-Ar geochronology). However, recent U-Pb dating of zircon yielded an age of 215± 4 Ma for the Dehnow granitoids (KARIMPOUR et al. 2010).

Analytical methods

Major oxide analyses of minerals were carried out using a wavelength-dispersive electron probe micro analyser, JEOL JXA-8800, at the Japanese Agency for Marine-Earth Science and Technology (JAMSTEC). The operating conditions were 15 kV accelerating voltage and 15 nA beam current. Standard corrections of atomic (Z) number factors (= ZAF) were performed. Natural and synthetic minerals of known composition were used as standards. The structural formula of epidote, biotite and plagioclase and ilmenite are calculated on the basis of, respectively, 12.5, 22, 8 and 12 oxygen atom per formula unit. The structural formula of amphibole is calculated based on 23 atoms of oxygen and 13-CNK ($CaO+Na_2O+K_2O$) cation normalization and charge balance. The average compositions and formula units of minerals in the Dehnow granitoids are given in Table 2 (see Appendix). Whole rock major element concentrations including nine major oxides (SiO_2, TiO_2, Al_2O_3, MnO, MgO, CaO, K_2O, Na_2O, P_2O_5) were measured on pressed powder tablets by X-ray fluorescence (XRF) using a Philips PW 1480 wavelength dispersive spectrometer with a Rh-anode X-ray tube and a 3 MeV electron beam Van de Graaff Accelerator, at the Geological Survey of Iran. The analyses have an uncertainty of 0.1 wt% and some selected trace elements have an uncertainty of 0.1 ppm. The quality of the analytical results was assessed by comparison with certified standard reference materials of GSP-2 prepared by the USGS. The trace element data were measured at the Activation Laboratories, Ontario, Canada (ActLabs). The whole rock samples were digested by lithium metaborate/tetraborate fusion and analysed with a Perkin Elmer Sciex ELAN 6000, 6100 or 9000 ICP/MS. Three blanks and five

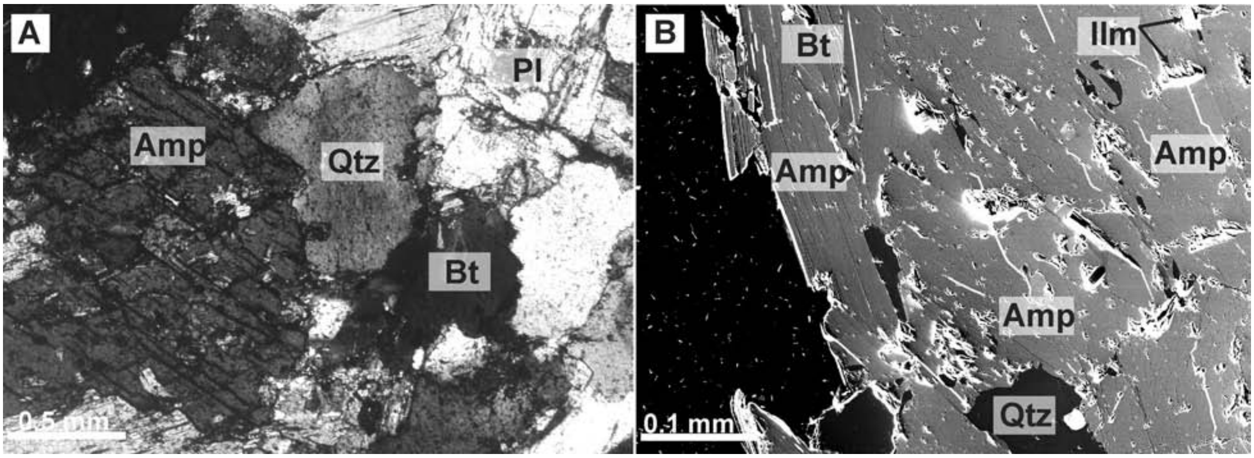

Fig. 2. A – Amphibole (Amp), biotite (Bt), quartz (Qtz) and plagioclase (Pl) in tonalite. Amphibole is replaced by biotite around the rims and fractures. **B –** Back-scatted image of amphibole and biotite with inclusions of quartz and ilmenite.

controls (three before each sample group and two after) were analysed per group of samples. Duplicates are fused and analysed every 15 samples. The instrument is recalibrated every 40 samples. The error for standards BIR-1a, W-2 and J-1 run with the samples is better than 5% relative to the certified values for the trace-elements and better than 1% for major element data (with the exception of Na_2O and MnO, which are better than 3%). The blanks ran with the samples were below the detection limit for all the elements reported. Whole-rock compositions of representative samples from Dehnow granitoids and surrounding micaschist are given in Table 3 (see Appendix).

Data and results

Mineralogy and mineral composition

The Dehnow pluton is medium-grained with a heterogeneous compositional range of diorite, tonalite to granodiorite. It is surrounded by micaschist and hornfels for which the protolith is interpreted to be shale. A narrow layer (~200 m) of hornfels developed in the contact aureole of this pluton. Following the emplacement of the pluton, low grade regional metamorphic activity led to the formation of a weak foliation in the intrusive rocks. The granitoid outcrops are dispersed in the area and the pluton is mostly covered by Quaternary gravel fan deposits (Fig. 1C). However, sampling was done from micaschist and hornfels at the contact zone, toward the inner outcrops of pluton in the south, east and west. After ~200 meters from the contact zone, diorite, tonalite and granodiorite were sampled. The granodiorite samples are mostly from the inner portions of the pluton that are selected from ~3 kilometers from the contact zone in the south. Samples from other locations are mostly tonalite (Fig. 1C). The DTG are dominated by a granular texture (Fig. 2). Sedimentary enclaves and metamorphic minerals (e.g. cordierite, sillimanite) are not found in the studied granitoid pluton. The modal composition of DTG is presented in Table 1 (see Appendix). Diorites and tonalites are composed of quartz, plagioclase (andesine to labradorite, Table 2; see Appendix), amphibole (ferro-hornblende to ferro-tschermakite hornblende, Fig. 3A), biotite (Fig. 3B) and alkali-feldspar as major igneous mineral phases, ilmenite, epidote and garnet as minor minerals, and smaller amounts of muscovite and chlorite as secondary minerals. Granodiorite is composed of quartz, plagioclase, alkali-feldspar and biotite as main mineral phases, and ilmenite, muscovite, garnet and amphibole as minor minerals. The biotites are characterized with average Fe/(Fe+Mg) of 0.60 and Al^{IV} of 2.51 a.p.f.u (Table 2). Some biotites formed at the expense of amphibole through the later metamorphism. Garnet has a widespread but rare occurrence through the pluton.

The hornfels consists of quartz, feldspar (albite to oligoclase), muscovite, biotite (with average Fe/(Fe+Mg) of 0.35 and Al^{IV} of 2.59 atom per formula unit), almandine-spessartine garnet, andalusite, chlorite, tourmaline, fibrolite and ilmenite. It has a porphyroblastic texture in which porphyroblasts of garnet

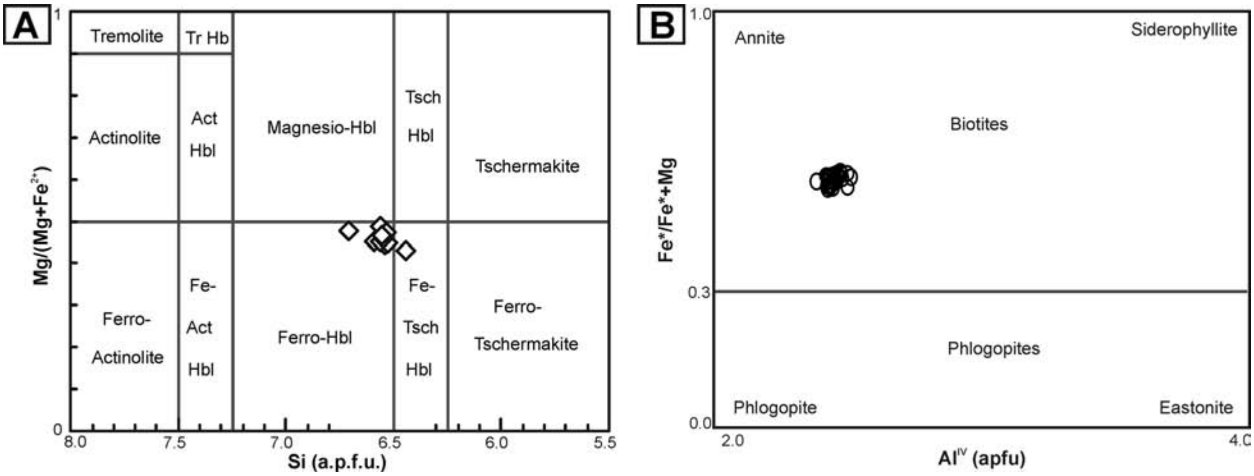

Fig. 3. Composition of: **A –** Amphibole based on the classification of HAWTHORNE & OBERTI (2007). **B –** Biotite based on the classification of DEER et al. (1992), in Dehnow DTG.

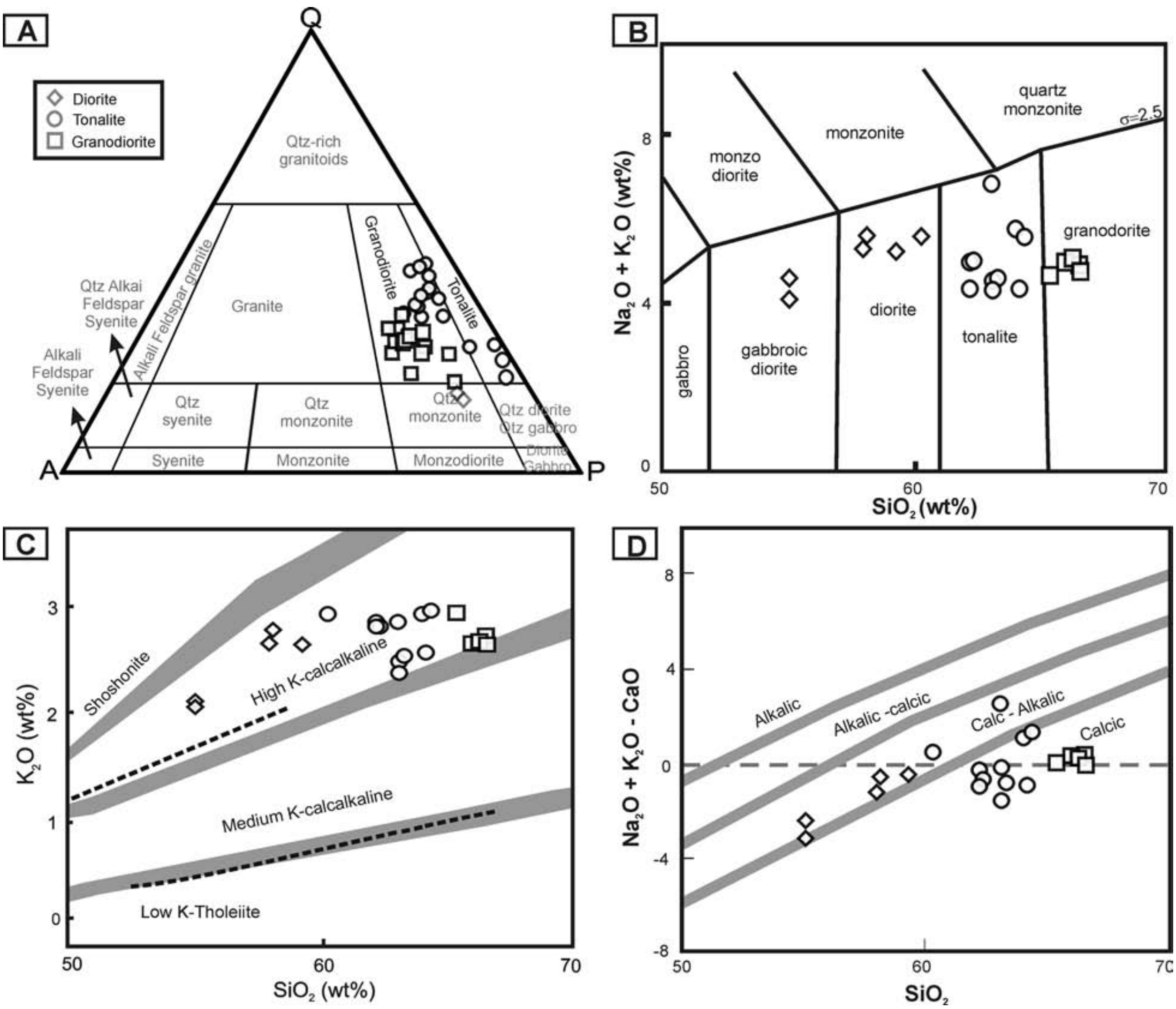

Fig. 4.

and andalusite are scattered through the fine-grained matrix. To the northwest of the margin of the Dehnow pluton, an outcrop of micaschist with a considerable topographic relief relative to the granitoid is present. The micaschist contains fewer felsic minerals than the hornfels and it is composed of quartz, alkali feldspar, plagioclase (albite-oligoclase), muscovite, biotite (characterized by average Fe/(Fe+Mg) of 0.32 and Al^{IV} of 2.68 atom per formula unit), almandine-spessartine garnet, andalusite, small euhedral to subhedral tourmaline, chlorite and ilmenite with a porphyroblastic texture.

Whole-rock geochemistry

The SiO_2 contents of Dehnow granitoids range from 55-59 wt% in diorite, 60-64 wt% in tonalite and 65-67 wt% in granodiorite. The modal composition indicates a diorite to tonalite and granodiorite composition (Fig. 4A). The alkali vs. silica diagram of Middlemost (1994) for the plutonic rocks suggest chemical compositions that range from diorite to tonalite and granodiorite (Fig. 4B). On the basis of the igneous spectrum of Hughes (1973) they are partially K-altered, thus showing a medium to high K-calc-alkaline affinity on the magmatic series K_2O versus SiO_2 discrimination diagram (Fig. 4C). According to the MALI index of Frost et al. (2001), the tonalite and granodiorites are calcic, whereas diorites are calc-alkalic (Fig. 4D). The major elements show variations from the granodiorite and tonalite towards diorite in the margin of the pluton with a negative correlation between the SiO_2 concentration and Al_2O_3, FeO, MnO, MgO and CaO contents. The Dehnow pluton shows enrichment of light rare earth element (LREE) and large ion lithophile elements (LILE) (Fig. 5A-B). It differs from the lower crust composition in Cs, Rb, Th, U, Nb, Ta, K and Pr concentrations (Fig. 5B). The samples lack concave-upward REE patterns, suggesting that amphibole and garnet were not involved in magma generation and segregation. The Ti, Pb and Y contents suggest differentiation from granodiorite, to tonalite and diorite. In addition, the LREE are more enriched in granodiorite and tonalite, whereas the heavy REE (HREE) are more enriched in the diorite (Fig. 5). Dehnow diorite has a $(La/Yb)_{cn}$ of 13.52-14.36, $(Tb/Yb)_{cn}$ of 1.54-1.64, $(La/Sm)_n$ of 4.02-4.20 and negative Eu anomalies (Eu/Eu* = 0.78-0.88), whereas the tonalite is characterized by higher $(La/Yb)_{cn}$ of 24.85, higher $(Tb/Yb)_{cn}$ of 2.17 and similar $(La/Sm)_n$ of 4.46 and negative Eu anomalies (Eu/Eu* = 0.88).

Karimpour et al. (2010) reported Sr and Nd radiogenic isotope compositions of Dehnow diorite as $^{87}Sr/^{86}Sr$ = 0.707949, $^{143}Nd/^{144}Nd$ = 0.512059, and ε_{Nd} = -5.9 and Mirnejad et al. (2013) obtained $^{87}Sr/^{86}Sr$ = 0.710905, $^{143}Nd/^{144}Nd$ = 0.512195, and ε_{Nd} = -6.1 for a tonalite sample (sample VA) and $^{87}Sr/^{86}Sr$ = 0.709889, $^{143}Nd/^{144}Nd$ = 0.512234, and ε_{Nd} = -5.5 for a diorite sample (sample VR). The $(^{87}Sr/^{86}Sr)_I$ values increase from diorite to tonalite whereas ε_{Nd} and $^{143}Nd/^{144}Nd$ decrease (Fig. 7).

Although the composition of the pluton is not homogenous, it drastically differs from the metapelites in composition. For example, the Fe_2O_3, Al_2O_3, and K_2O contents are higher in hornfels and micaschists, whereas CaO, MgO, Na_2O and P_2O_5 are lower in comparison. The hornfels have a $(La/Yb)_{cn}$ of 12.519, $(Tb/Yb)_{cn}$ of 1.423 and negative Eu anomalies of 0.732. The micaschist samples have lower $(La/Yb)_{cn}$ of 10.464 and 9.969, and similar $(Tb/Yb)_{cn}$ of 1.457 and 1.274 and negative Eu anomalies of 0.694 and 0.703. In contrast, Dehnow micaschists and hornfels have REE patterns that resemble those of the North American shale composite and the average upper crust, with the exception of their being depleted in Ba and Sr, and enriched in Sm and Y (Fig. 5C).

Discussion

P-T conditions of magma crystallization

The Al-in-hornblende geobarometer is based on the total Al-content in magmatic hornblende buffered by the eight-phase assemblage plagioclase+K-feldspar+quartz+biotite+epidote or magnetite+rutile+ilmenite+melt (Schmidt & Poli 2004). The calculated pressures

Fig. 4. Discrimination diagrams for the Dehnow granitoids. **A –** Modal QAP diagram of Streckeisen (1974). **B –** Total alkalis vs. silica (TAS) vs. SiO_2 classification diagram for plutonic rocks (after Middlemost 1994). **C –** K_2O vs. SiO_2 magmatic series diagram from Rickwood (1989) and Peccerillo & Taylor (1976). **D –** Na_2O+K_2O-CaO vs. SiO_2 diagram of Frost et al. (2001).

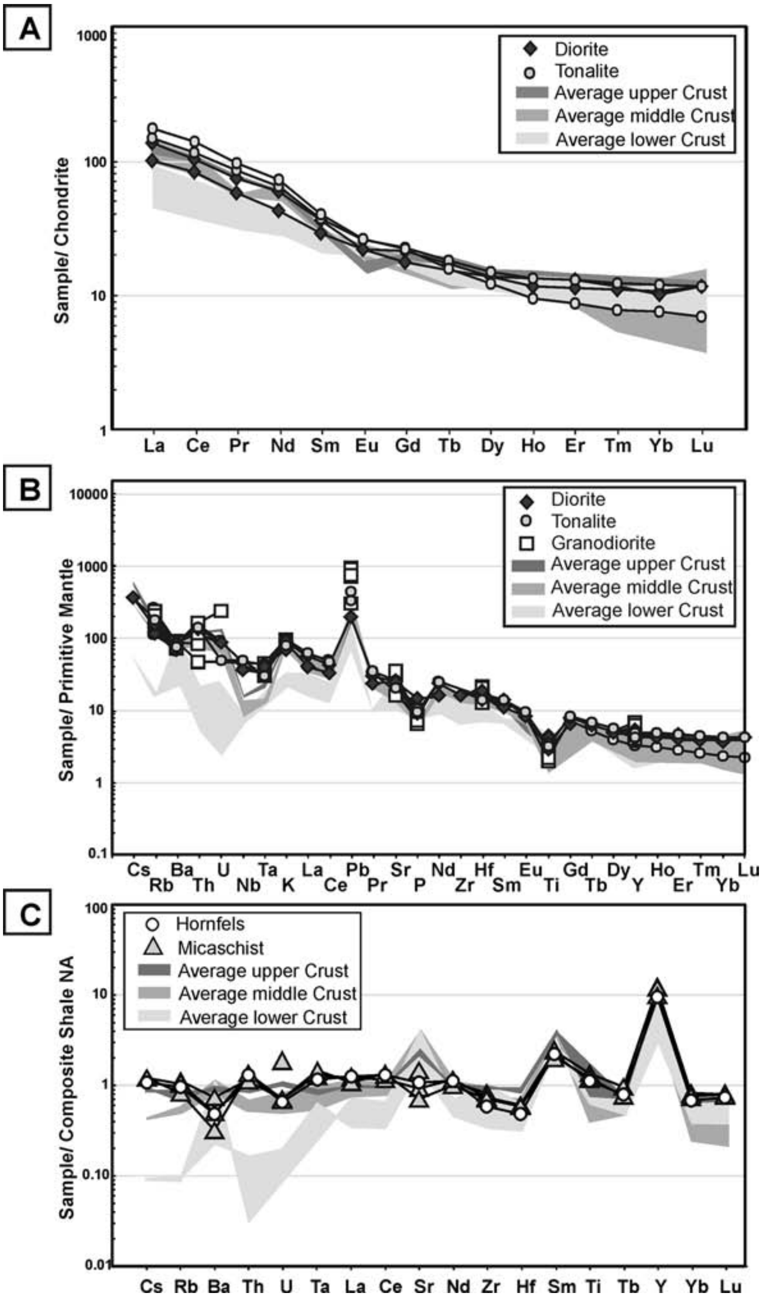

Fig. 5. A – Chondrite-normalized trace element patterns for Dehnow granitoids. **B –** Primitive mantle-normalized patterns. **C –** North American composite shale-normalized patterns for Dehnow micaschist and hornfels. The average lower crust values are from Weaver & Tarney (1984) and Taylor & McLennan (1985, 1995), average middle crust values are from Weaver & Tarney (1984) and Rudnick & Gao (2003), and average upper crust from Taylor & McLennan (1985, 1995) and Rudnick & Gao (2003).

are 6.2, 6.6 and 6.6 kbar using the calibrations of Hammarstrom & Zen (1986), Hollister et al. (1987) and Schmidt (1992), respectively. Amphibole-plagioclase thermometry of DTG based on the calibration by Blundy & Holland (1990), based on the reaction of: edenite+4quartz = tremolite+albite, indicates a temperature of ~700 ± 7 °C. The average calculated P-T values correspond to emplacement and crystallization in

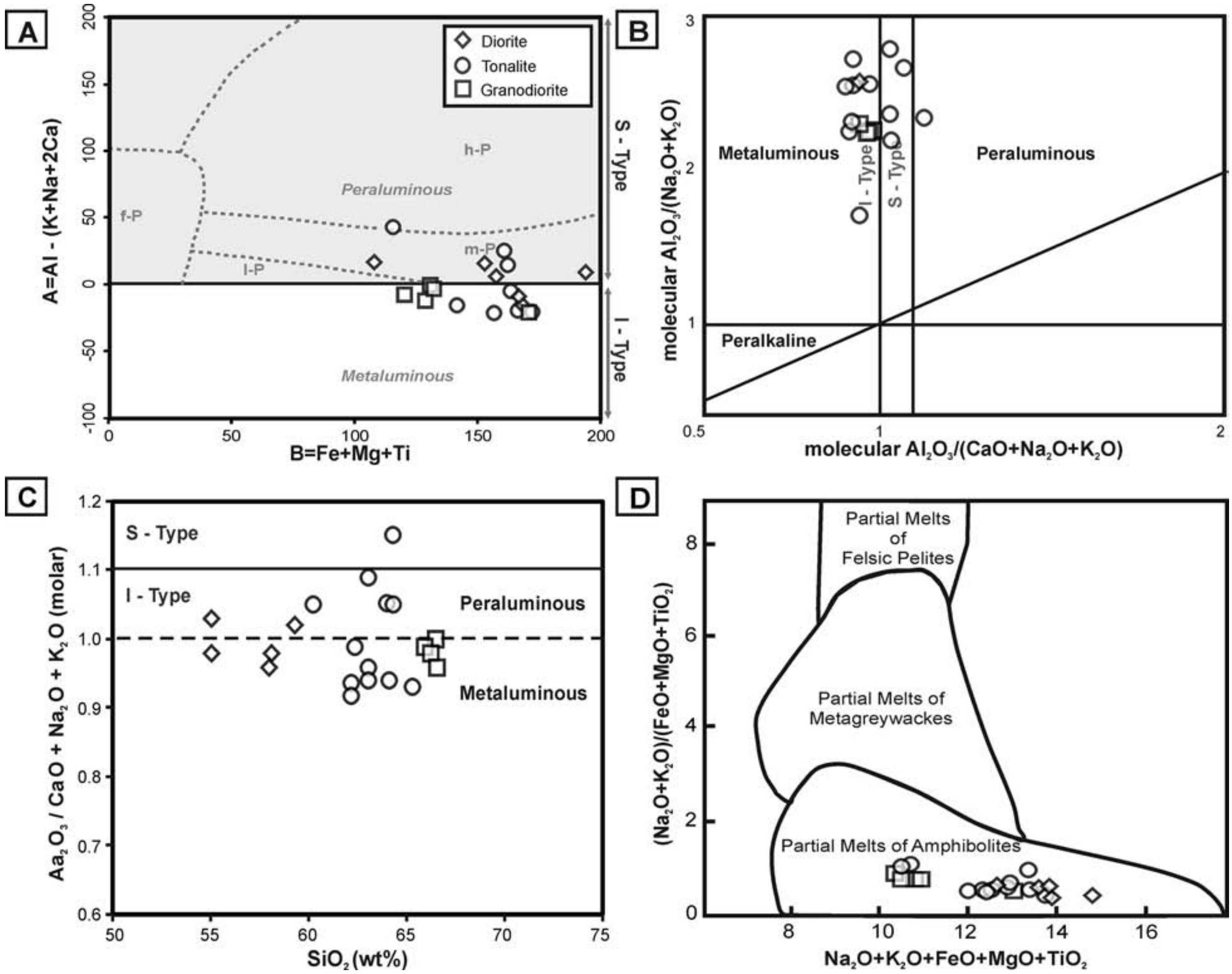

Fig. 6. Discrimination diagrams for the Dehnow granitoids. **A –** A-B diagram (Debon & Le Fort 1983) with fields of various types of peralkaline rocks as outlined by Villaseca et al. (1998). Boundary line of I- and S-type granitoids is drawn based on data from the Lachlan Fold Belt (White & Chappell 1989). FP = highly felsic peraluminous granitoid, HP = highly peraluminous granitoid, MP = moderately peraluminous granitoid, LP = low peraluminous granitoid. **B –** Molecular $Al_2O_3/(Na_2O+K_2O)$ vs. molecular $Al_2O_3/(CaO+Na_2O+K_2O)$ diagram (Maniar & Piccoli 1989). **C –** Molecular $Al_2O_3/CaO+Na_2O+K_2O$ vs. SiO_2 diagram. **D –** $(Na_2O+K_2O)/(FeO+MgO+TiO_2)$ vs. $Na_2O+K_2O+FeO+MgO+TiO_2$ plot (Almeida et al. 2007).

the upper lithosphere and they confirm that the equilibrium condition of amphibole and plagioclase crystallization was ~6.4 kbar, ~700 °C at a depth of ca. 22 km. Experimental petrology (Rutter & Wyllie 1988; Skjerlie & Johannes 1996; Singh & Johannes 1996) reveals that partial melting of dry tonalitic rocks in the upper lithosphere (~20 kbar) leads to the production of tonalites. The heat required was caused by crustal thikkening as intrusives cool (i.e. latent heat of fusion) or by thermal conduction from mafic magmas from the mantle wedge that underplated, or were emplaced within the continental crust (e.g. Huppert & Sparks 1988). On the basis of P-T diagrams of Ti-bearing phases of Liu et al. (1996), the presence of ilmenite in the Dehnow DTG indicates emplacement conditions of P<12 kbar and T>750 °C. This is also confirmed by the occurrence of epidote. Its average pistacite component (Ps = 0.18, Table 2) and low TiO_2 contents (<0.17%) suggest that epidote is a primary mineral according to the criteria of Evans & Vance (1987). The presence of such magmatic epidote inclusions in magmatic amphibole endorsed the primacy of epidote crystallization. According to Schmidt & Poli (2004), the appearance of epidote before hornblende during the crystallization history of a cooling DTG magma may occur below 10 kbar. The temperature calculated by amphibole-hornblende thermometry is not the highest temperature limit at which melt crystallized, but it is the temperature at which plagioclase and hornblende have simultaneously formed and equilibrated. Therefore, during magma ascent and emplacement of the pluton, the crystallization succession epidote, amphibole, plagioclase occurred over an approximate pressure range that decreased from >12 to ~6 kbar and at temperatures decreasing to an average temperature of 700 °C, i.e. the equilibrium temperature of plagioclase and hornblende.

I-type affinity

As Chappell & White (2001) suggested, the I- and S-type subdivision is not simply one that reflects different compositions, but also refers to source rocks of fundamentally different origins involving prior infracrustal and supracrustal origins. For both I- and S-type granites, melting of the source rocks at minimum temperatures results in a slightly peraluminous composition known as the "minimum-melt" composition (Chappell & White 1992). In this case, the magma or "minimum-melt" plus restite will initially have the same composition as that of the crustal source material. As the mantle is the ultimate source of all I-type granites, with fractional crystallization and/or restite separation, a range of compositions between "minimum-melt" and mantle-derived material is produced (Chappell et al. 1998; Chappell 1999). Partial melting of metapelitic and upper crustal sources is not admissible for the Dehnow magma, because no mineralogical or geochemical correlation was found between Dehnow granitoids and surrounding metapelites. The higher amount of Ca-bearing minerals (e.g. plagioclase, amphibole, epidote, etc.) in the granitoids led to lower alumina saturation indices (A/CNK) (= molar Al_2O_3/(CaO+Na_2O+K_2O), Na_2O/CaO and Rb/Ba ratios compared to those of the metapelites. While the metapelitic samples are mostly enriched in K-rich feldspars and micas, Rb/Ba, Zr, Zn, V, Rb, and Y values also show a smooth decrease toward the granitoid margins but distinctly increase in the hornfels and schists (Table 3, see Appendix). The I-Type affinity and magmatic source of the Dehnow granitoid is discussed in the following paragraphs.

The presence of magmatic amphibole is an indicator of I-type magma by Barbarin (1999) and amphibole in the Dehnow pluton is within the compositional range of hornblendes in I-Type granites studied by Zen (1986). Based on the MgO-Al_2O_3 discrimination diagram (Fig. 2 in Villaseca et al. 2009), the biotite composition (MgO~8.33 and Al_2O_3~16.50) supports an I-type affinity of the host rock as well.

The aluminum saturation index of the Dehnow samples is 0.47 and that of the I-Type granite of Zen (1986) is 0.33-0.70. There are no large, discrete apatite crystals, which are known to be common in S-type granites as described by Chappell & White (1974). The lack of enclaves of supracrustal origin in those granites, apart from xenoliths of local country rock, is further evidence that the source rocks of the Dehnow granitoids were infracrustal I-type granites Chappell & White (2001). While the S-type granites are restricted to higher SiO_2 contents (>60 wt%), Dehnow granitoids have a broad spectrum of compositions from diorite to tonalite and granodiorite that can be attributed to an I-type granitoid sequence (Chappell & White 1974). The compositions of the Dehnow granitoid samples lie in the metaluminous to peraluminous field, with an A/CNK of 0.93-1.05, indicating their I-type nature as do the discriminant diagrams of Al-(K+Na+2Ca) vs. Fe+Mg+Ti, molecular Al_2O_3/(Na_2O+K_2O) vs. molecular Al_2O_3/(CaO+Na_2O+K_2O) and Al_2O_3/CaO+Na_2O+K_2O vs. SiO_2 (Fig. 6A-B-C). According to the (Na_2O+K_2O)/(FeO+MgO+TiO_2) vs. Na_2O+K_2O+FeO+MgO+TiO_2 diagram, the Dehnow granitoids may derive by partial melting of amphibolite (metabasalt) in the source (Fig. 6D). Experimental studies of Chappell et al. (2012) showed that clinopyroxene and other Ca components in the source can dissolve in the melt at higher temperatures of partial melting, with the melt eventually becoming metaluminous. The later K-alteration effects may have partially caused the high potassium content of these rocks (Fig. 6C) as we mentioned before. However, even if the source rocks contained less than 50% of the current K_2O content (~1 wt%), the A/CNK ratio did not significantly increase, as is common for S-type granitoids (i.e. A/CNK>1). Following Chappell et al. (2012), the absence of older, inherited zircon in the Dehnow samples support the high temperature I-type character of the granitoid. Chappell & White (1992) suggested that I-type granites have initial $^{87}Sr/^{86}Sr$ ranging from 0.704 to 0.712 and ε_{Nd} ranging from -3.5 to -8.9. For batholithic S-type granites the corresponding values are 0.708 to 0.717 and -5.8 to -8.8. However, there is

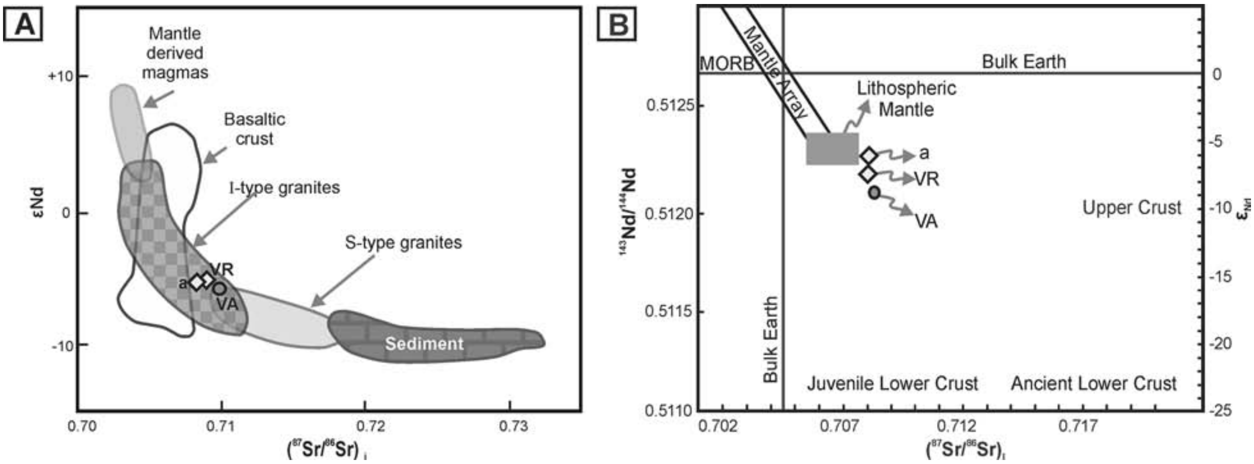

Fig. 7. A. Plot of ε_{Nd} versus initial Sr isotope ratios by Keay et al. (1997) in Dickin (2005). **B –** $^{143}Nd/^{144}Nd$ vs. $(^{87}Sr/^{86}Sr)_i$ plot of Dehnow diorite (data for sample "a" is from Karimpour et al. (2010) and samples "VR" (diorite) and "VA" (tonalite) data are from Mirnejad et al. 2013).

a large overlap between the initial Sr and Nd isotope compositions of I- and S-type granitoids, with continuity in $^{87}Sr/^{86}Sr$ from 0.704 to 0.720. Chappell & White (2001) concluded that the cause of overlap is not known, but proposed that it was the result of derivation from a range of source rocks comprising various proportions of igneous and sedimentary material. The $^{87}Sr/^{86}Sr$ and ε_{Nd} value of the Dehnow diorite and tonalite samples plot within the I-type granitic field (Fig. 7A), with an affinity closer to the lower crust rather than upper crust (Fig. 7B).

On the other hand, apart from the typically medium-grained and equigranular textures, the presence of mafic minerals such as amphibole and biotite and the metaluminous and calc-alkaline compositions connect the Dehnow granitoids to Cordilleran and Caledonian, both I-type, granites. Although the Dehnow pluton is partially zoned from a basic margin of diorite or tonalite to an acid core of granodiorite, as is known for the I-type Cordilleran granites (Cobbing 2000), it shows some other features of Caledonian I-type granites. For instance, their distribution is scattered and the volume is small, they have a high K metaluminous and calc-alkaline composition and moderate $^{87}Sr/^{86}Sr$ values (from 0.707 to 0.710) suggesting a crustal component in the melt source (Cobbing 2000). In addition, the low temperatures obtained by amphibole-hornblende thermometry (~708 °C) are similar to the Caledonian granites or the low-temperature I-type granitoids of Chappell et al. (1998).

Magma genesis and tectonic setting

Petrography and geochemistry of the samples show that the Dehnow pluton is an amphibole-rich calc-alkaline granitoid (ACG). Tectonic reconstructions and geochemical evidence also suggest that the setting in which these granitoids were generated was one of oceanic-continental lithosphere convergence, where mantle melts interacted with the overriding lithosphere. On the ternary plot of Maniar & Piccoli (1989), it is ascribed to a POG (post-orogenic granitoid) tectonic setting (Fig. 8A) within a normal continental arc (Fig. 9B). The Nb vs. Y and Rb vs. Yb+Ta discriminant diagrams of Pearce et al. (1984) suggest a volcanic arc granitoid nature for the Dehnow granitoids (Fig. 8C-D). On the basis of the geological scheme by Zanchi et al. (2011), the Mashhad granitoids were emplaced in the Turan Plate, within the Mashhad-Pamir Arc, during the Late Triassic collision of the Central Iran Plate with Eurasia and during closure of the Paleo-Tethys.

Williams et al. (1992) noted that "zircons with inherited cores are rare in I-type granites, but virtually every zircon in the S-types contains an older core". The U-Pb results of Karimpour et al. (2010) also suggest an igneous origin for the dated zircons and a non-sedimentary origin for their host rock, because they did not report any inherited cores. Furthermore, if the zircons originated from the surrounding Paleo-Tethys metasedimentary rocks, they must have yielded much older ages.

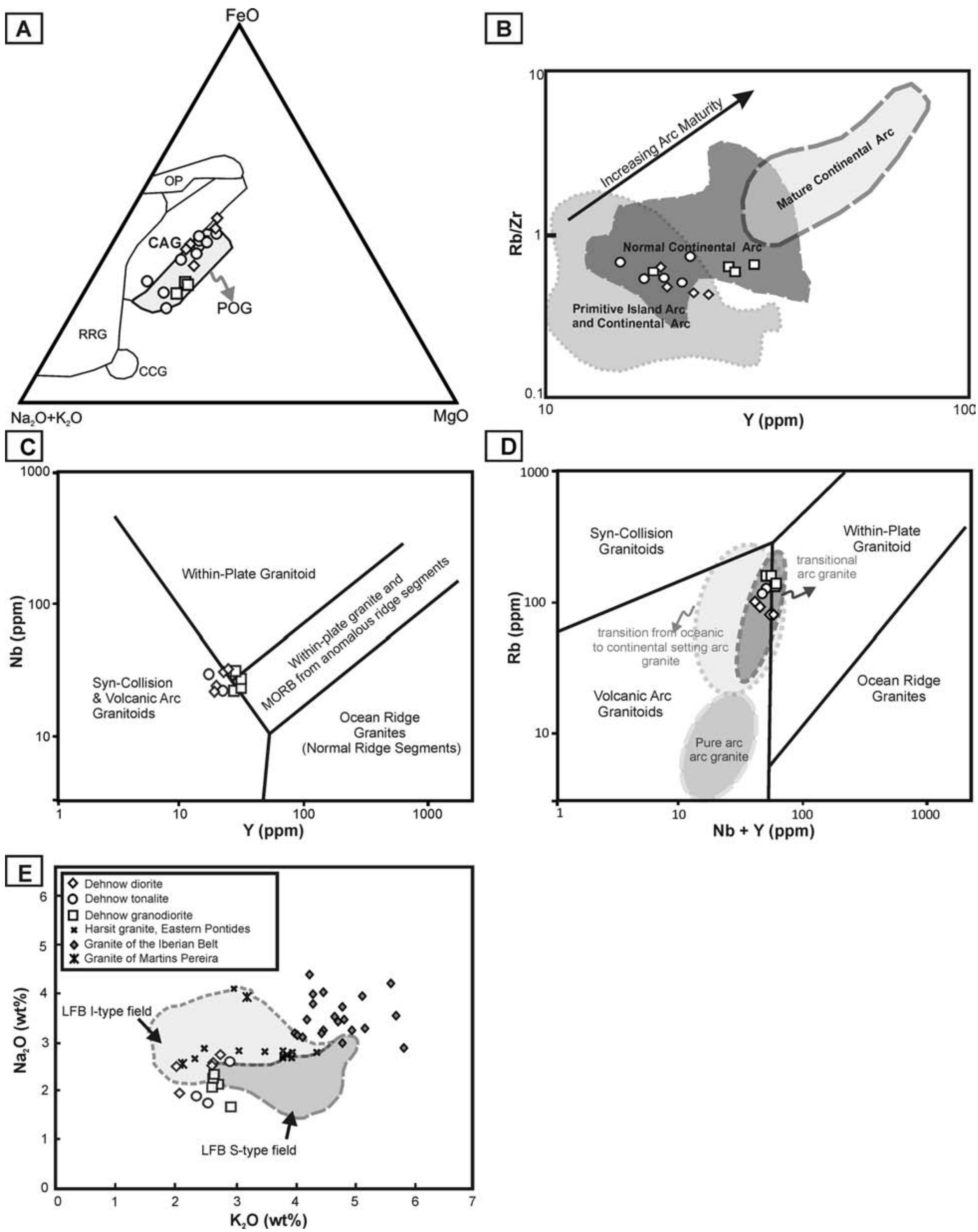

Fig. 8. A. Diorite, Tonalite and Granodiorite samples on the AFM discriminant ternary diagram of Maniar & Piccoli (1989). **B –** Rb/Zr versus Y discriminant diagram of (Brown et al. 1984). **C –** Nb versus Y discriminant diagram of (Pearce et al. 1984). **D –** Rb versus Yb+Ta discriminant diagram (after Pearce et al. 1984). **E –** Na_2O vs. K_2O plot showing compositional data of S-type and I-type granites from the Lachlan Folded Belt (LFB). The data of the I-type granites are from Harsit, Iberian and Martins Pereira areas are from Karsli et al. (2010); Villaseca et al. (2009) and Almeida et al. (2007), respectively.

Global comparison with other I-type granitoids

I-type granitoids are orogenic granites of mixed origin (mantle plus crust) and are chemically consistent with collisional metaluminous potassic calc-alkaline granites, post-collisional metaluminous potassic calc-alkaline granites and metaluminous calc-alkaline granites in subduction zones (Barbarin 1990). The two main tectonic environments envisaged for high-K magma generation are (a) continental arc (Cordilleran- or Andean-type) (Roberts & Clemens 1993), and (b) post-collisional (Caledonian-type) settings (Almeida et al. 2007). Cordilleran I-types granitoids are generally considered to be subduction-related, occur at the borders of major continents and are more highly evolved than M-types (mantle derived granite). Although they are principally tonalitic and granodioritic, they also contain a proportion of monzogranite. However, post-collisional I-type granitoids provide a bimodal association consisting predominantly of monzogranites and granodiorites in association with minor basic intrusives, and may also occur in close association with S-types which may be structurally separated, as in the Lachlan Fold Belt and the Scottish Caledonides (Cobbing 2000). In this section we compare the trace elements of the Dehnow granitoids with some examples of orogenic (I-type) granites from elsewhere:

(1) Metaluminous to peraluminous, high K - low Ca, I-type granitoids from a collisional setting from Martins Pereira in southeastern Roraima State, Brazil (Almeida et al. 2007). Almeida et al. (2007) pointed out that an ancient plutonic collisional magmatic event (1.97-1.96 Ga) was represented by I-type high-K calc-alkaline granitoids. These were probably generated from crustal sources by partial melting, most likely during amalgamation of the tonalite-trondhjemite-granodiorite (TTG) -like Anaua magmatic arc with the Transamazon and Central Amazonian terranes.

(2) Peraluminous to metaluminous, high K - low Ca, I-type granites from the post-collisional setting of the Variscan Iberian Belt in southwestern Europe (Villaseca et al. 2009). For the Iberian terranes, Villaseca et al. (2009) proposed that oceanic lithosphere and therefore, metabasic or related rocks were involved in the genesis of post-tectonic granitic melts. However, they suggested that the presence of I-type granites could be related to differences in composition of the protoliths involved in the partial melting processes.

(3) Metaluminous, high K, I-type granitoids from a pre- plate collisional, subduction zone setting in Harsit, in the western portion of the Alpine-Himalayan fold-and-thrust belt (Karsli et al. 2010). The Harsit magma is known to have formed in a back-arc extensional environment resulting in the opening of the East Black Sea Basin. The geochemical data show that assimilation of upper crustal material appears plausible during the generation of this pluton (Karsli et al. 2010).

The Dehnow granitoids, as well as these granitoids, are clearly excluded from the S-type granites of the LFB (SE Australia), but are comparable with I-type granites of the LFB (Fig. 8E). Dehnow granitoids also differ from S-type granites from Serra Dourada (in Brazil) (Almeida et al. 2007) by having higher concentrations of HREE, Th, U, Pr and Eu and lower concentrations of LREE, Y and Ti (Fig. 9A-B). The compared granitoids share similar trace and rare earth element signatures on the chondrite- and primitive mantle- normalized diagrams (Fig. 9). The general pattern similarity of these elements for the Dehnow granitoids and the I-type granitoids from Harsit, Martins Pereira and Iberia, characterized by high LREE contents, high field strength element (HFSE) depletion and flat HREE, are due to their I-type affinity (Fig. 9C-H). A negative Eu anomaly is common for Harsit, Martins Pereira and Iberia granitoids, but Dehnow samples show no Eu anomaly. The Dehnow granitoids contrast with the Harsit pluton in having lower Th and HREE and higher LREE, Pb, Ti, Nb, U, Ta contents. It also shows some negligible differences with Martins Pereira pluton in having lower Th, U, Ti, Hf and lacking a Eu anomaly, and with the Iberian plutons in having lower Th, U and HREE and higher Pr, Sr, U, Nb, Ta, Zr and Ti contents. Chondrite-normalized REE patterns confirm that the Dehnow granitoids geochemically most resemble the collisional I-type tonalite to monzogranite of Martins Pereira (Fig. 9A-C-E-G). Bulk rock compositions of the Mashhad granitoids suggest an arc-related setting that developed on a continental crust and finally ceased due to the collision of the Iranian and Turanian micro-plates in early Jurassic times. Zanchi et al. (2011) interpreted these units as remnants of a suprasubduction arc-related complex, grown during the Permian along the active Eurasian margin above a north-dipping subduction zone, where the Paleo-Tethys Ocean was consumed.

Conclusions

1. Based on major and trace element compositions in combination with published isotope data; the Dehnow granitoids are metaluminous and I-type calcalkaline and formed in a subduction setting, with a close affinity to the lower crust and mantle melts.

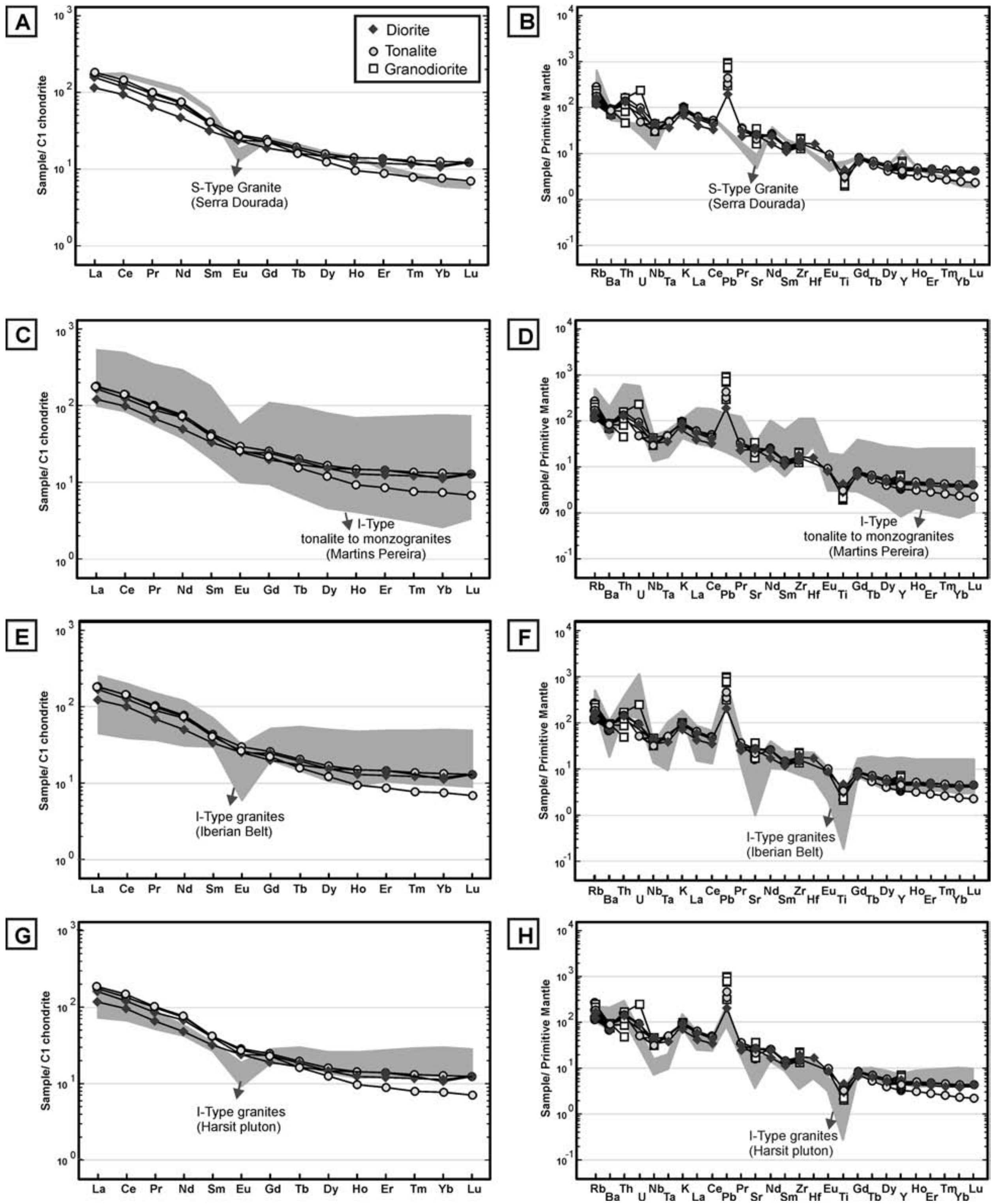

Fig. 9. Dehnow diorite, tonalite and granodiorite compositions plotted as: **A**, **C**, **E**, **G,** C1 chondrite-normalized pattern, **B**, **D**, **F**, **H** primitive mantle normalized. The data for I-type Martins Pereira tonalite to monzogranite and S-type Serra Dourada granite are from ALMEIDA et al. (2007). The data of I-type granites from the Harsit and Iberian areas are from KARSLI et al. (2010), and VILLASECA et al. (2009), respectively.

2. The whole rock and mineral compositions as well as the lack of sedimentary enclaves and absence of metamorphic minerals (e.g. cordierite, sillimanite) in the studied granitoid pluton indicate that the magma source may not be related to the metasedimentary country rocks.
3. The chemistry of the Dehnow granitoids is similar to some worldwide high-K, calc-alkaline, I-type granites as, for example, from Harsit along the Alpine-Himalayan suture zone, Martins Pereira, and Iberia, in that all are characterized by high LREE and low HFSE contents and flat HREE patterns. It is most analogous to the metaluminous to peraluminous high K-low Ca I-type granitoids from the collisional setting of Martins Pereira and is least analogous to metaluminous high K I-type granitoids from pre-plate collisional setting of a subduction zone from Harsit pluton.
4. A subduction-related origin of the Dehnow granitoids is also supported by its 215 ± 4 Ma, Late Triassic U-Pb zircon crystallization age (Karimpour et al. 2010) in combination with the Devonian-Carboniferous age of deposition of the protoliths of the metaflysch country rocks (Majidi 1981). Therefore, the absence of inherited, sedimentary zircon in the studied granitoids indicates that the magma was not generated by partial melting of Paleozoic flysch and other clastic sediments in the area.
5. P-T calculations using amphibole-plagioclase thermometry and hornblende barometry reveal crystallization stages within the upper lithosphere at an approximate pressure of 6.4 kbar and an approximate temperature of 708 °C. Such low P-T conditions characterize them as Caledonian-type granitoids, which is supported by petrographical and geochemical features such as the small size and scattered distribution of the plutons, their high-K metaluminous and calc-alkaline compositions and moderate $^{87}Sr/^{86}Sr$ ratios.
6. The geochemical data suggest that the Dehnow pluton is an arc-related granitoid that developed along the active Eurasian margin, above and on a north-dipping subduction zone that finally ceased due to the collision of the Iranian and Turanian micro-plates in Early Jurassic times.

Acknowledgements

We thank the Institute for Research on Earth Evolution (Yokosuka, Japan). The authors express gratitude to the constructive reviews of Ian Saginor and Allan Collins and the editorial handling of associated editor Martin Timmerman which improved the original manuscript. We sincerely thank Jarek Trela for his helpful review of the manuscript. The bulk rock and major and trace element data was supported in part by Virginia Tech start-up to EG.

References

Alavi, M. & Majidi, B. (1972): Petrology and geology of metamorphic and intrusive rocks of the Mashhad area. – Geological Survey of Iran, Tehran, 30 pp.
Alavi, M. (1991): Sedimentary and structural characteristics of the Paleo-Tethys remnants in northeastern Iran. – Geological Society of America Bulletins, **103** (8): 983-992.
Alberti, A. & Moazez-Lesco, Z. (1974): Plutonic and metamorphic rocks of the Mashhad area (Khorasan, North-Eastern Iran). – Bollettino della Società Geologica Italiana, **93**: 1157-1196.
Almeida, M.E., Macambira, M.J.B. & Oliveira, E.C. (2007): Geochemistry and zircon geochronology of the I-type high-K calc-alkaline and S-type granitoid rocks from southeastern Roraima, Brazil: Orosirian collisional magmatism evidence (1.97-1.96 Ga) in central portion of Guyana Shield. – Precambrian Research **155**: 69-97.
Barbarin, B.A. (1990): Granitoids: main petrogenetic classifications in relation to origin and tectonic setting. – Geological Journal, **25**: 227-238.
Barbarin, B.A. (1999): Review of the relationships between granitoid types, their origin and their geodynamic environments. – Lithos, **46**: 605-626.
Berberian, F. (1981): Petrogenesis of Iranian plutons: A study of the Natanz and Bazman intrusive complex. – 300 pp.; PhD thesis, University of Cambridge.
Blundy, J.D. & Holland, T.J.B. (1990): Calcic amphibole equilibria and a new amphibole-plagioclase geothermometer. – Contributions to Mineralogy and Petrology, **104**: 208-224.
Brown, G.C., Thorpe, R.S. & Webb, P.C. (1984): The geochemical characteristics of granitoids in contrasting arcs and comments on magma sources. – Journal of the Geological Society of London, **141**: 413-26.
Chappell, B.W. & White, A.J.R. (1974): Two contrasting granite types. – Pacific Geology, **8**: 173-174.
Chappell, B.W. & White, A.J.R. (1984): I- and S-type granites in the Lachlan Fold Belt, southeastern Australia. – In: Keqin, X. & Guangchi, T. (Eds.): Geology of Granites and Their Metallogenic Relations, 87-101; Beijing (Science Press).
Chappell, B.W. & White, A.J.R. (1992): I- and S-type granites in the Lachlan Fold Belt. – Transactions of the Royal Society of Edinburgh Earth Sciences, **83**: 1-26.
Chappell, B.W. & White, A.J.R. (2001): Two contrasting granite types, 25 years later. – Australian Journal of Earth Sciences, **48**: 489-499.
Chappell, B.W. (1999): Aluminum saturation in I- and S-type granites and the characterization of fractionated haplogranites. – Lithos, **46**: 535-551.
Chappell, B.W., Bryant, C.J. &Wyborn, D. (2012): Peraluminous I-type granites. – Lithos, **153**: 142-153.
Chappell, B.W., Bryant, C.J., Wyborn, D., White, A.J.R. & Williams, I.S. (1998): High- and low-temperature I-type granites. – Resource Geology, **48**: 225-236.

Cobbing, J. (2000): The geology and mapping of granite batholiths. – 141 pp.; Berlin, Heidelberg (Springer).
Debon, F. & Le Fort, P. (1983): A chemical-mineralogical classification of common plutonic rocks and associations. – Transactions of the Royal Society of Edinburgh Earth Sciences, **73**: 135-149.
Deer, W.A., Howie, R.A. & Zussman, J. (1992): An Introduction to the Rock forming Mineral. – 696 pp.; 2nd ed., London (Longman).
Dickin, A.P. (2005): Radiogenic Isotope Geology. – 493 pp.; 2nd ed., Cambridge (University Press).
Evans, B.W. & Vance, J.A. (1987): Epidote phenocrysts in dacitic dikes, Boulder country. – Contributions to Mineralogy and Petrology, **96**: 178-185.
Frost, B.R., Barnes, C.G., Collins, W.J., Arculus, S.R.J., Ellis, D.J. & Frost, C.D. (2001): A geochemical classification for granitic rocks. – Journal of Petrology, **42**: 2033-2048.
Gill, R. (2010): Igneous Rocks and Processes: A practical guide. – 428 pp.; Hoboken (Wiley-Blackwell).
Haghipour, A. & Aghanabati, A. (1989): Geological Map of Iran: scale 1:2,500,000. – 2nd ed., Geological Survey of Iran, Tehran.
Hammarstrom, J.M. & Zen, E. (1986): Aluminum in hornblende: An empirical igneous geobarometer. – American Mineralogist, **71**: 1297-1313.
Hawthorne, F.C. & Oberti, R. (2007): Classification of the Amphiboles. – Reviews in Mineralogy and Geochemistry, **67**: 55-88.
Hollister, L.S., Grissom, G.C., Peters, E.K., Stowell, H. & Sisson, V.B. (1987): Confirmation of the empirical correlation of Al in hornblende with pressure of solidification of calc-alkaline plutons. – American Mineralogist, **72**: 231-239.
Hughes, C.J. (1973): Spilites, keratophyres, and the igneous spectrum. – Geological Magazine, **109**: 513-527.
Huppert, H.E. & Sparks, S.J. (1988): The generation of granitic magmas by intrusion of basalt into continental crust. – Journal of Petrology, **29**: 599-624.
Iranmanesh, J. & Sethna, S.F. (1998): Petrography and geochemistry of the Mesozoic granite at Mashhad, Khorasan Province, northeastern part of Iran. – Journal of the Geological Society of India, **52(1)**: 87-94.
Jamshidi-Bahr, M., Collins, A.S., Masoudi, F., Cox, G. & Mohajel, M. (2013): The U-Pb age, geochemistry and tectonic significance of granitoids in the Soursat Complex, northwest Iran. – Turkish Journal of Earth Sciences, **22**: 1-31.
Karimpour, M.H., Stern, C.R. & Farmer, L. (2010): Zircon U-Pb geochronology, Sr-Nd isotope analyses, and petrogenetic study of the Dehnow quartz diorite and Kuhsangi granodiorite (Paleo-Tethys), NE Iran. – Journal of Asian Earth Sciences, **37**: 384-393.
Karsli, O., Dokuz, A., Uysal, I., Aydin, F., Chen, B., Kandemir, R. & Wijbrans, J. (2010): Relative contributions of crust and mantle to generation of Campanian high-K calc-alkaline I-type granitoids in a subduction setting, with special reference to the Harşit Pluton, Eastern Turkey. – Contributions to Mineralogy and Petrology, **160** (4): 467-487.
Keay, S., Collins, W.J. & McCulloch, M.T. (1997): A three component Sr-Nd isotopic mixing model for granitoid genesis, Lachlan fold belt, eastern Australia. – Geology, **25**: 307-310.
Lammerer, B., Langheinrich, G. & Manutchehr-Danai, M.M. (1984): Geological Investigation in the Binalud Mountain (NE Iran). – Neues Jahrbuch für Geologie und Paläontologie, Abhandlungen, **168**: 269-277.
Liu, J., Bohlen, S.R. & Ernest, W.G. (1996): Stability of hydrous phases in subducting oceanic crust. – Earth and Planetary Science Letters, **143**: 161-171.
Majidi, B. (1978): Etude petrostructural de la region de Mashhad (Iran), Les problems de metamorphites, serpentinites et granitoides Hercynians. – 277 pp.; These Universite Scientifique et Medicale de Grenoble, France.
Majidi, B. (1981): The ultrabasic lava flow of Mashhad, NE-Iran. – Geological Magazine, **118**: 49-58.
Majidi, B. (1983): The geochemistry of ultrabasic and basic lava flow occurrence in Northeast Iran. – Geodynamic project (Geotravers) in Iran. Geological Survey of Iran, **51**: 463-477.
Maniar, P.D. & Piccoli, P.M. (1989): Tectonic discrimination of granitoids. – Geological Society of America, Bulletins, **101**: 635-643.
Middlemost, E.A.K. (1994): Naming materials in the magma/igneous rock system. – Earth Science Reviews, **37**: 215-224.
Mirnejad, H. (1991): Geochemistry and petrography of Mashhad granites and pegmatites. – 250 pp.; M.Sc. Thesis, University of Tehran, Tehran, Iran.
Mirnejad, H., Lalonde, A.E., Obeid, M. & Hassanzadeh, J. (2013): Geochemistry and petrogenesis of Mashhad granitoids: An insight into the geodynamic history of the Paleo-Tethys in northeast of Iran. – Lithos, **170-171**: 105-116.
Moazez-Lesco, Z. & Plimer, I.R. (1979): Intrusive and Polymetamorphic Rocks of the Darakht-Bid Area, near Mashhad, Iran. – Geologische Rundschau, **68**: 318-383.
Natalin, B.A. & Sengor, A.M.C. (2005): Late Palaeozoic to Triassic evolution of the Turan and Scythian platforms: The pre-history of the Palaeo-Tethyan closure. – Tectonophysics, **404**: 175-202.
Pearce, J.A., Harris, N.B.W. & Tindle, A.G. (1984): Trace element discrimination diagrams for the tectonic interpretation of granitic rocks. – Journal of Petrology, **25**: 956-983.
Peccerillo, A. & Taylor, S.R. (1976): Geochemistry of Eocene calcalkaline volcanic rocks from Kastamonu area, northern Turkey. – Contributions to Mineralogy and Petrology, **56**: 221-246.
Pitcher, W.S. (1993): The nature and origin of granite. – 387 pp.; London (Chapman and Hall).
Rahimi, B. & Alizadeh, H. (2010): Structural analysis, origin and deformation conditions of ductile shear zones in Dehnow granitoid pluton-West of Mashhad. – Iranian Journal of Crystallography and Mineralogy, **18** (3): 397-408.
Rickwood, P.C. (1989): Boundary lines within petrologic diagrams which use oxides of major and minor elements. – Lithos, **22**: 247-267.
Rudnick, R.L. & Gao, S. (2003): The Composition of the Continental Crust. – In: Holland, H.D. & Turekian,

K.K. (Eds.): Treatise on Geochemistry, **3**: 1-64; Oxford (Elsevier-Pergamon).
Rutter, J.M. & Wyllie, P. (1988): Melting of vapor-absent tonalite at 10 Kb to simulate dehydration-melting in the deep crust. – Nature, **331**: 159-160.
Roberts, M.P. & Clemens, J.D. (1993): The origin of high-K, calc-alkaline, I-type granitoid magmas. – Geology, **21**: 825-828.
Samadi, R. (2009): The origin of garnet megacrysts from Dehnow Tonalite, Northwest of Mashhad. – 179 pp.; M.Sc. Thesis, University of Tehran, Tehran, Iran.
Samadi, R. (2014): Chemistry and origin of garnet in the granitoids and metamorphic rocks in the south of Mashhad (Khajeh-Morad, Khalaj and Dehnow). – 300 pp.; Ph.D. Thesis, Tehran Science and Research Branch, Islamic Azad University, Tehran, Iran.
Samadi, R., Valizadeh, M.V., Mirnejad, H. & Kawabata, H. (2012): Geothermometry and geobarometry of metamorphic rocks of Dehnow (Northwest of Mashhad). – Journal of Geosciences, **21** (84): 3-14.
Samadi, R., Mirnejad, H. & Kawabata, H., Harris, C., Valizadeh, M.V. & Gazel, E. (2014): Magmatic garnet in the Triassic (215 Ma) Dehnow pluton of NE Iran and its petrogenetic significance. – International Geology Review, **56** (05): 596-621.
Schmidt, M.W. & Poli, S. (2004): Magmatic Epidote. – Reviews in Mineralogy and Geochemistry, **56**: 399-430.
Schmidt, M.W. (1992): Amphibole composition in tonalite as a function of pressure: An experimental calibration of the Al-in-hornblende barometer. – Contributions to Mineralogy and Petrology, **110**: 304-310.
Sheikholeslami, M.R. & Kouhpeyma, M. (2012): Structural analysis and tectonic evolution of the eastern Binalud Mountains, NE Iran. – Journal of Geodynamics, **61**: 23-46.
Singh, J. & Johannes, W. (1996): Dehydration melting of tonalites. Part 2: composition of melt and solid. – Contributions to Mineralogy and Petrology, **125**: 26-44.
Skjerlie, K.P. & Johanson, A.D. (1996): Vapour-absent melting from 10 to 20 kbar of crustal rocks that contain multiple hydrous phases: implications for anatexis in the deep to very deep continental crust and active continental margins. – Journal of Petrology, **37**: 661-691.
Soltani, A. (2000): Geochemistry and geochronology of I type granitoid rocks in the northeastern central Iran. – 300 pp.; PhD thesis, School of Geosciences, University of Wollongong, Australia.
Streckeisen, A.L. (1974): Classification and Nomenclature of Plutonic Rocks. Recommendations of the IUGS Subcommission on the Systematics of Igneous Rocks. – Geologische Rundschau, **63**: 773-785.
Taylor, S.R. & McLennan, S.M. (1985): The continental crust: Its composition and evolution. – 312 pp.; Oxford (Blackwell).
Taylor, S.R. & McLennan, S.M. (1995): The geochemical evolution of the continental crust. – Reviews of Geophysics, **33** (2): 241-265.
Valizadeh, M.V. & Karimpour, M.H. (1995): Petrogenesis of Mashhad granites and granodiorites and their tectonic setting. – Journal of Science of University of Tehran, **21** (1): 71-82.
Villaseca, C., Barbero, L. & Rogers, G. (1998): Crustal origin of Hercynian peraluminous granitic batholiths of central Spain: petrological, geochemical and isotopic (Sr, Nd) constraints. – Lithos, **43**: 55-79.
Villaseca, C., Bellido, F., Pérez-Soba, C. & Billström, K. (2009): Multiple crustal sources for post-tectonic I-type granites in the Hercynian Iberian Belt. – Mineralogy and Petrology, **96**: 197-211.
Weaver, B.L. & Tarney, J. (1984): Empirical approach to estimating the composition of the continental crust. – Nature, **310**: 575-577.
White, A.J.R. & Chappell, B.W. (1989): Geology of the Numbla 1:100 000. – Sheet 8624; Geological Survey of New South Wales, Sydney.
Williams, I.S., Chappell, B.W., Chen, Y.D. & Crook, K.A.W. (1992): Inherited and detrital zircons – vital clues to the granite protoliths and early igneous history of southeastern Australia. – Transactions of the Royal Society of Edinburgh: Earth Sciences, **83**: 503.
Zanchi, A., Berra, F., Balini, M., Ghassemi, M.R., Heidarzadeh, G. & Zanchetta, S. (2011): The Palaeotethys Suture Zone in NE Iran: New Constraints on the Evolution of the Eo-Cimmerian Belt (Darius Programme). – Proceeding of AAPG International Conference and Exhibition, Milan, Italy.
Zen, E. (1986): Aluminum enrichment in silicate melts by fractional crystallization: some mineralogic and petrographic constraints. – Journal of Petrology, **27**: 1095-1117.

Manuscript received: October 26th, 2013.
Revised version accepted by the Potsdam editor: January 24th, 2014.

Addresses of the authors:

Ramin Samadi (corresponding author), Seyed Jamal Sheikh Zakariaee, Department of Geology, College of Basic Sciences, Tehran Science and Research Branch, Islamic Azad University, Tehran, Iran;
e-mail: rsamadi@hotmail.com

Esteban Gazel, Department of Geosciences, Virginia Tech, 4044 Derring Hall (0420), Blacksburg, VA 24061, USA

Hassan Mirnejad, Department of Geology, Faculty of Science, University of Tehran, Tehran, Iran

Hiroshi Kawabata, Research and Education Faculty, Kochi University, Kochi 780-8520, Japan

Ali Akbar Baharifar, Department of Geology, Payame Noor University, I.R. of Iran

Appendix

Table 1. Modal mineralogy of the Dehnow granitoids (Qtz = quartz, Pl = plagioclase, Amp = amphibole, Bt = biotite, Ep^1 = epidote replacing plagioclase, Ep^2 = epidote replacing biotite, Ep^3 = magmatic epidote, Ms = muscovite replacing amphiboles, Myr = myrmekite, Cpx = clinopyroxene, Sph = sphene, Ap = apatite, Zr = zircon, Ala = alanite, other = sum of muscovite, zircon, garnet, apatite, chlorite, opaque etc in some samples).

Rock Type	Thin Section	Qtz	Pl	Kfs	Amp	Bt	Ep^1	Ep^2	Ep^3	Ms	Myr	Cpx	Sph	Ap	Zr	Ala	other
Granodiorite	GD2.1	23.5	40.3	13.9	6.9	13.0	-	-	-	-	-	-	-	-	-	-	2.4
	GD2.2	21.3	43.1	12.2	10.1	12.0	-	-	-	-	-	-	-	-	-	-	1.8
	GD1.1	23.0	39.7	14.1	5.7	15.0	-	-	-	-	-	-	-	-	-	-	2.9
	GD1.2	20.6	35.0	11.2	9.2	21.0	-	-	-	-	-	-	-	-	-	-	3.8
	TD-4	24.4	42.4	10.6	10.9	8.8	-	-	-	-	-	-	-	-	-	-	3.0
	H12*	16.6	54.1	11.4	-	16.5	-	-	-	0.4	0.2	-		0.5	0.3	-	-
	H8*	29.5	45.0	16.8	-	6.1	-	-	-	1.9	0.1	-	0.1	0.5	-	-	-
	H21*	23.0	46.0	12.5	-	15.8	-	-	-	0.7	0.6	-	0.6	0.5	0.1	0.2	-
	H27*	30.6	41.8	14.0	-	12.8	-	-	-	-	-	-	0.2	0.2	0.1	0.2	-
	N43*	21.0	49.2	9.2	-	15.1	-	-	-	0.1	3.9	-	-	1.1	0.3	-	-
	R23*	18.5	47.2	17.6	-	12.8	-	-	-	-	2.7	-	0.1	0.6	0.3	0.2	-
	H23*	26.2	44.9	14.9	-	13.1	-	-	-	-	0.6	-	-	-	0.1	-	-
	H34*	28.2	41.4	17.8	-	10.1	-	-	-	-	0.6	-	1.2	-	0.3	-	-
	H40*	21.0	39.8	17.7	-	17.5	-	-	-	0.1	3.5	-	-	0.2	0.2	-	-
	R17*	24.5	41.8	17.1	-	16.0	-	-	-	0.2	-	-	0.1	0.2	0.1	-	-
Tonalite	T-1*	15.3	43.8	1.0	22.0	17.0	-	-	-	-	-	-	-	-	-	-	1.8
	T-3*	13.0	47.0	2.0	15.0	18.3	-	-	-	-	-	-	-	-	-	-	4.9
	T2*	27.3	41.2	10.0	0.1	15.5	1.2	1.4	1.1	0.4	1.9	-	-	0.6	0.2	-	-
	T5*	38.2	38.5	4.6	-	13.0	2.1	1.7	1.0	0.6	-	-	-	0.2	-	-	-
	T6*	28.1	38.3	9.1	-	22.0	1.2	0.3	0.2	0.6	-	-	-	0.1	-	-	-
	T12*	28.9	38.3	9.6	0.6	17.2	2.8	1.6	0.1	0.8	-	-	-	0.1	-	-	-
	M2*	30.1	37.9	6.4	-	22.9	1.3	0.8	0.1	0.1	0.3	-	-	-	-	-	-
	M41*	32.7	40.2	6.2	-	18.3	1.1	0.3	0.7	0.4	-	-	-	0.1	-	-	-
	W17*	31.3	39.4	8.1	1.0	17.1	1.6	0.8	0.2	-	0.5	-	-	-	-	-	-
	W31*	34.6	38.8	5.1	-	16.8	1.6	2.2	0.2	0.8	-	-	-	-	-	-	-
	L21*	27.6	44.3	6.5	-	16.6	2.9	0.2	0.2	0.9	0.6	-	-	0.1	-	-	-
	L12*	35.1	35.2	7.3	-	15.3	3.2	1.8	0.7	1.4	-	-	-	-	-	-	-
	L42*	25.5	34.7	11.1	-	14.6	1.1	2.1	0.1	1.3	0.4	-	-	0.1	-	-	-
	T41*	30.0	30.3	4.6	1.5	29.0	1.6	0.9	0.1	0.1	-	1.0	-	0.1	0.1	-	-
	T46*	28.5	39.4	5.2	0.9	23.2	1.3	0.4	-	0.4	0.3	0.3	-	-	-	-	-
	T52*	17.2	39.6	4.2	9.0	25.2	1.2	1.3	0.2	-	-	2.0	-	-	0.1	-	-
	T71*	20.2	49.1	1.3	2.1	25.4	0.6	1.2	-	0.1	-	-	-	-	-	-	-
Diorite	DH-2011a	11.0	48.5	9.5	9.0	16.0	-	-	-	-	-	-	-	-	-	-	4.0
	DH-2011b	12.0	48.3	10.1	10.0	15.2	-	-		-	-	-	-	-	-	-	4.5

* data from Mirnejad (1991)

Table 2. Averages of representative mineral compositions from Dehnow DTG, hornfels and micaschist (n: Analytical points for each mineral, Mg# = Mg/(Mg+Fe^{2+}), Fe# = Fe/(Fe+Mg), Ps = Fe^{3+}/(Fe^{3+}+Al)).

Rock Type	DTG					Hornfels				Micaschist			
Mineral Type	Pl	Amp	Ep	Bt	Ilm	Pl	Bt	Grt	Ilm	Pl	Bt	Grt	Ilm
Sample no.	9	2	2	10	9	4	4	9	4	4	4	13	8
SiO_2	54.69	42.71	38.76	35.64	0.36	64.38	37.32	37.07	2.58	64.63	33.82	36.93	4.77
TiO_2	0.01	1.03	0.12	2.52	52.19	0.00	1.02	0.14	51.24	0.03	1.93	0.13	46.93
Al_2O_3	28.27	11.19	27.61	16.50	0.24	21.81	26.72	21.44	2.03	21.49	19.73	21.38	7.58
Cr_2O_3	0.00	0.01	0.00	0.01	0.00	0.00	0.06	0.01	0.02	0.00	0.03	0.02	0.01
FeO	0.11	20.62	6.79	21.86	43.73	0.20	15.58	34.91	41.17	0.35	23.34	36.54	38.48
MnO	0.00	0.65	0.42	0.38	2.43	0.00	0.13	4.85	0.91	0.01	0.07	3.22	0.72
MgO	0.01	7.27	0.03	8.33	0.18	0.03	4.85	1.85	0.10	0.03	6.20	1.90	0.19
CaO	10.52	11.42	22.87	0.06	0.16	1.79	0.04	0.38	0.00	1.94	0.19	0.41	0.03
Na_2O	5.53	0.99	0.12	0.08	0.02	10.18	0.65	0.03	0.03	10.47	0.31	0.02	0.02
K_2O	0.08	1.10	0.01	9.12	0.01	0.26	7.38	0.00	0.07	0.11	7.28	0.01	0.09
Total	99.23	97.01	96.74	94.50	99.33	98.65	93.75	100.66	98.15	99.04	92.90	100.55	98.82
Oxygen	8	23	13	22	12	8	22	12.00	12	8	22	12.00	12
Si	2.48	6.51	3.03	5.50	0.04	2.87	5.41	1.62	0.25	2.88	5.33	1.72	0.44
Al	1.51	2.01	2.54	3.00	0.03	1.15	4.53	0.24	0.23	1.12	3.66	0.85	0.82
Al^{iv}	-	1.49	-	2.50	-	-	2.59	0.13	-	-	2.68	0.44	-
Al^{vi}	-	0.52	-	0.50	-	-	1.94	1.01	-	-	0.99	1.01	-
Ti	0.00	0.12	0.01	0.29	3.97	0.00	0.12	1.86	3.82	0.00	0.23	1.66	3.36
Cr	0.00	0.00	0.00	0.00	0.00	0.00	0.01	0.00	0.00	0.00	0.00	0.00	0.00
Fe	0.00	2.63	0.44	2.82	3.69	0.01	1.93	3.31	3.42	0.01	3.07	3.00	3.07
Fe^{3+}	-	0.50	0.44	-	-	0.01	-	0.34	-	0.01	-	0.18	-
Fe^{2+}	-	2.13	-	-	-	-	-	2.50	-	-	-	2.56	-
Mn	0.00	0.08	0.03	0.05	0.21	0.00	0.02	0.22	0.08	0.00	0.01	0.15	0.06
Mg	0.00	1.65	0.00	1.92	0.03	0.00	1.08	0.12	0.01	0.00	1.46	0.13	0.03
Ca	0.51	1.86	1.91	0.01	0.02	0.09	0.01	0.02	0.00	0.09	0.03	0.02	0.00
Na	0.49	0.29	0.02	0.02	0.00	0.88	0.18	0.00	0.01	0.90	0.10	0.00	0.00
K	0.00	0.21	0.00	1.80	0.00	0.02	1.38	0.00	0.01	0.01	1.46	0.00	0.01
Sum	5.01	15.37	7.98	15.41	7.99	5.00	19.31	7.80	7.83	5.02	15.44	7.84	7.79
Mg#	-	0.44	-	-	-	-	-	0.05	-	-	-	0.05	-
Fe#	-	0.49	-	-	-	-	-	-	-	-	-	-	-
Ps	-	-	0.15	-	-	-	-	-	-	-	-	-	-
Albite	0.48	-	-	-	-	89.74	-	-	-	90.16	-	-	-
Anorthite	0.51	-	-	-	-	8.75	-	-	-	9.25	-	-	-
Orthose	0.00	-	-	-	-	1.52	-	-	-	0.59	-	-	-
Almandine	-	-	-	-	-	-	-	71.76	-	-	-	83.76	-
Pyrope	-	-	-	-	-	-	-	6.69	-	-	-	7.67	-
Grossular	-	-	-	-	-	-	-	0.57	-	-	-	1.13	-
Spessartine	-	-	-	-	-	-	-	20.98	-	-	-	7.39	-
Andradite	-	-	-	-	-	-	-	0.00	-	-	-	0.00	-
Uvarovite	-	-	-	-	-	-	-	0.02	-	-	-	0.06	-

Table 3. Comparative XRF and ICP-MS data of Dehnow granodiorite, tonalite, diorite, hornfels and micaschist.

Rock Type	Granodiorite					Tonalite					
Sample no.	TD4	GD2.2	GD1.1	GD2.1	GD1.2	T5*	TD1	TD-1*	TD-3*	VA*	TD3
SiO_2	65.37	65.98	66.25	66.50	66.60	63.07	63.12	63.12	63.31	64.01	64.18
Al_2O_3	13.21	14.74	15.02	14.54	14.32	16.49	15.18	15.76	16.65	16.92	14.25
$Fe_2O_3^{(T)}$	7.37	5.21	4.68	5.09	4.98	5.61	7.07	7.02	7.21	5.17	7.07
FeO	5.28	3.34	2.86	3.23	3.13	3.70	5.01	4.97	5.14	3.30	5.01
Fe_2O_3	2.09	1.87	1.82	1.86	1.85	1.91	2.06	2.05	2.07	1.87	2.06
MnO	0.14	0.11	0.11	0.10	0.12	0.21	0.13	0.12	0.15	0.11	0.13
MgO	2.56	2.28	2.12	2.28	2.29	2.31	2.14	2.32	2.34	1.32	2.52
CaO	4.61	4.62	4.81	4.52	4.80	4.28	5.86	4.70	5.43	4.64	5.29
Na_2O	1.62	2.22	2.29	2.09	2.03	3.86	1.85	1.98	1.98	2.72	1.71
K_2O	2.93	2.63	2.65	2.71	2.62	2.84	2.35	2.45	2.51	2.91	2.54
TiO_2	0.72	0.50	0.43	0.49	0.46	0.73	0.69	0.67	0.62	0.48	0.69
P_2O_5	0.21	0.16	0.16	0.14	0.16	0.27	0.23	0.21	0.26	0.17	0.23
LOI	1.15	0.96	1.25	1.08	1.09	1.12	1.22	1.29	1.28	1.44	1.19
Total	99.9	99.4	99.8	99.5	99.5	100.8	99.8	99.6	101.7	99.9	99.8
Na_2O/CaO	0.35	0.48	0.48	0.46	0.42	0.90	0.32	0.42	0.36	0.59	0.32
A/CNK	0.9	1.0	1.0	1.0	1.0	1.0	0.9	1.1	1.1	1.1	0.9
A/NK	2.3	2.3	2.3	2.3	2.3	1.7	2.7	2.7	2.8	2.2	2.6
V	65	117	99	110	115	-	76	76	71	28	71
Cr		3		4	6	-	8	8	-	54	-
Co	9	29	33	31	24	-	13	-	-	-	9
Ni	2	18	4	40	-	-	3	3	2	4	2
Rb	82	150	126	151	132	-	86	86	83	120	83
Sr	335	734	687	734	727	487	486	486	441	420	441
Y	18	31	31	27	28	-	21	21	19	15	19
Zr	140	236	196	241	226	-	172	-	-	178	153
Nb		23	27	22	31	-		-	-	32	
Mo	-	-	-	-	-	-	-	-	-	-	-
Cs	-	-	-	-	-	-	-	-	-	-	-
Ba	509	513	605	619	625	624	475	475	518	574	518
La	-	-	-	-	-	-	-	-	-	43.53	-
Ce	-	-	-	-	-	-	-	-	-	88.87	-
Pr	-	-	-	-	-	-	-	-	-	9.37	-
Nd	-	-	-	-	-	-	-	-	-	34.58	-
Sm	-	-	-	-	-	-	-	-	-	6.09	-
Eu	-	-	-	-	-	-	-	-	-	1.50	-
Gd	-	-	-	-	-	-	-	-	-	4.39	-
Tb	-	-	-	-	-	-	-	-	-	0.58	-
Dy	-	-	-	-	-	-	-	-	-	2.99	-
Ho	-	-	-	-	-	-	-	-	-	0.52	-
Er	-	-	-	-	-	-	-	-	-	1.38	-
Tm	-	-	-	-	-	-	-	-	-	0.19	-
Yb	-	-	-	-	-	-	-	-	-	1.19	-
Lu	-	-	-	-	-	-	-	-	-	0.17	-
Hf	-	-	-	-	-	-	-	-	-	-	-
Ta	-	-	-	-	-	-	-	-	-	2.00	-
Pb	21	68	65	51	52	-	23	-	-	-	31
Bi	-	-	-	-	-	-	-	-	-	-	-
Th		14.0	10.0	7.0	4.0	-	-	-	-	14.0	-
U		5.00	-	-	-	-	1.00	-	-	2.00	-
Sr/Y	18.611	23.677	22.161	27.185	25.964		23.143	23.143	23.211	28.000	23.211
Rb/Ba	0.161	0.292	0.208	0.244	0.211		0.181	0.181	0.160	0.209	0.160
Eu/Eu*	-	-	-	-	-	-	-	-	-	0.884	-
$(La/Yb)_{cn}$	-	-	-	-	-	-	-	-	-	24.850	-
$(La/Sm)_{cn}$	-	-	-	-	-	-	-	-	-	4.464	-
$(La/Lu)_{cn}$	-	-	-	-	-	-	-	-	-	26.578	-
$(Tb/Yb)_{cn}$	-	-	-	-	-	-	-	-	-	2.174	-

Table 3. Continued.

Rock Type	Diorite								
Sample no.	T2*	V-6**	V5**	V-2**	V-1**	DH-2011-1	VR*	TD- 2*	TD- 4*
SiO_2	64.37	55.12	55.10	58.16	59.32	58.02	60.31	62.23	62.39
Al_2O_3	17.17	19.02	18.65	18.14	17.59	18.07	17.45	14.89	16.57
$Fe_2O_3^{(T)}$	4.30	8.59	8.65	7.44	6.36	7.51	6.68	7.32	6.87
FeO	2.52	6.38	6.43	5.34	4.37	5.41	4.66	5.24	4.83
Fe_2O_3	1.78	2.21	2.22	2.10	1.99	2.10	2.02	2.08	2.04
MnO	0.16	0.20	0.16	0.16	0.14	0.15	0.13	0.14	0.14
MgO	2.11	2.70	3.01	2.32	2.60	2.31	2.20	2.54	2.51
CaO	4.19	7.25	6.99	6.13	5.69	6.50	5.10	5.23	5.67
Na_2O	2.49	1.90	2.46	2.71	2.48	2.53	2.55	2.01	2.09
K_2O	2.95	2.07	2.02	2.76	2.62	2.63	2.91	2.84	2.79
TiO_2	0.46	0.92	0.96	0.76	0.62	0.77	0.69	0.83	0.72
P_2O_5	0.22	0.23	0.32	0.22	0.20	0.21	0.21	0.27	0.22
LOI	1.01	2.05	1.86	1.55	1.50	1.37	1.82	1.32	1.26
Total	99.4	100.1	100.2	100.4	99.1	100.1	100.1	99.6	101.2
Na_2O/CaO	0.59	0.26	0.35	0.44	0.44	0.39	0.50	0.38	0.37
A/CNK	1.2	1.0	1.0	1.0	1.0	1.0	1.1	0.9	1.0
A/NK	2.4	-	-	-	-	2.6	2.4	2.3	2.6
V	-	-	-	-	-	102	70	78	65
Cr	-	-	-	-	-	20	35	-	-
Co	-	-	-	-	-	9	-	-	-
Ni	-	-	-	-	-	20	4	8	2
Rb	178	76	75	102	96	87	113	72	82
Sr	564	537	533	540	514	520	540	378	335
Y	-	22	24	-	19	19	22	17	18
Zr	-	177	178	205	154	187	154	-	-
Nb	-	31	32	29	22	24	22	-	-
Mo	-	-	-	-	-	2	-	-	-
Cs	-	-	-	-	-	3	-	-	-
Ba	567	470	466	594	576	613	597	529	509
La	-	-	-	-	28.06	39.10	41.59	-	-
Ce	-	-	-	-	58.90	75.80	83.42	-	-
Pr	-	-	-	-	6.22	8.06	9.20	-	-
Nd	-	-	-	-	22.31	31.60	33.91	-	-
Sm	-	-	-	-	4.83	6.07	6.19	-	-
Eu	-	-	-	-	1.37	1.38	1.61	-	-
Gd	-	-	-	-	3.85	4.75	4.98	-	-
Tb	-	-	-	-	-	0.68	0.72	-	-
Dy	-	-	-	-	3.66	3.73	4.06	-	-
Ho	-	-	-	-	-	0.69	0.79	-	-
Er	-	-	-	-	2.27	1.95	2.24	-	-
Tm	-	-	-	-	-	0.29	0.33	-	-
Yb	-	-	-	-	1.77	1.85	2.09	-	-
Lu	-	-	-	-	-	0.31	0.31	-	-
Hf	-	-	-	-	-	4.90	-	-	-
Ta	-	-	-	-	-	1.50	2.00	-	-
Pb		-	-	-	-	14	-	-	-
Bi	-	-	-	-	-	0.1	-	-	-
Th	-	-	-	-	-	11.3	12.0	-	-
U	-	-	-	-	-	1.79	1.00	-	-
Sr/Y		23.970	22.020	-	27.490	26.804	24.545	22.235	18.611
Rb/Ba	0.314	0.160	0.160	0.170	0.170	0.142	0.189	0.136	0.161
Eu/Eu*	-	-	-	-	-	0.783	0.884	-	-
$(La/Yb)_{cn}$	-	-	-	-	-	14.358	13.518	-	-
$(La/Sm)_{cn}$	-	-	-	-	-	4.023	4.196	-	-
$(La/Lu)_{cn}$	-	-	-	-	-	13.177	13.926	-	-
$(Tb/Yb)_{cn}$	-	-	-	-	-	1.639	1.536	-	-

Table 3. Continued.

Rock Type	Hornfels	Micaschist		
Sample no.	DH-2011-4	Sch-D	DH-2011-2	DH-2011-3
SiO_2	56.91	52.28	62.88	59.91
Al_2O_3	21.57	20.56	18.64	19.31
$Fe_2O_3^{(T)}$	10.04	15.57	9.09	11.58
FeO	7.68	12.66	6.83	9.07
Fe_2O_3	2.36	2.91	2.26	2.51
MnO	0.14	0.16	0.21	0.16
MgO	1.59	1.69	1.58	1.77
CaO	0.32	0.59	0.36	0.35
Na_2O	1.19	0.66	0.99	0.59
K_2O	2.20	2.58	2.42	1.74
TiO_2	0.86	0.90	1.06	0.95
P_2O_5	0.07	0.09	0.13	0.09
LOI	3.66	4.09	3.37	3.11
Total	98.6	99.2	100.7	99.6
Na_2O/CaO	3.72	1.12	2.75	1.69
A/CNK	4.4	4.2	3.8	5.5
A/NK	5.0	5.3	4.4	6.8
V	103	127	136	128
Cr	110	116	100	120
Co	21	27	31	25
Ni	60	47	50	80
Rb	121	138	132	104
Sr	154	207	134	101
Y	21	26	25	21
Zr	115	166	147	142
Nb	19	-	22	22
Mo	2	-	2	2
Cs	6	-	6	6
Ba	305	463	319	202
La	38.70	-	38.20	33.90
Ce	86.90	-	78.10	89.30
Pr	7.90	-	8.26	7.08
Nd	30.60	-	32.30	27.30
Sm	5.88	-	6.48	5.35
Eu	1.24	-	1.35	1.12
Gd	4.53	-	5.43	4.41
Tb	0.67	-	0.81	0.66
Dy	3.86	-	4.80	4.01
Ho	0.73	-	0.92	0.75
Er	2.11	-	2.55	2.18
Tm	0.32	-	0.36	0.33
Yb	2.10	-	2.48	2.31
Lu	0.34	-	0.37	0.36
Hf	3.00	-	3.80	3.70
Ta	1.29	-	1.44	1.62
Pb	22	27	25	32
Bi	0.3	-	0.2	0.3
Th	15.8	-	13.8	16.8
U	1.77	5.00	1.85	1.87
Sr/Y	7.512	7.962	5.296	4.856
Rb/Ba	0.397	0.298	0.414	0.515
Eu/Eu*	0.732	-	0.694	0.703
$(La/Yb)_{cn}$	12.519	-	10.464	9.969
$(La/Sm)_{cn}$	4.110	-	3.681	3.957
$(La/Lu)_{cn}$	11.920	-	10.775	9.856
$(Tb/Yb)_{cn}$	1.423	-	1.457	1.274